



Sveriges lantbruksuniversitet
Swedish University of Agricultural Sciences

Department of Forest Mycology and Plant
Pathology

A window to the future of Sweden's pine forestry?

Development of declining Scots pine after a
severe drought and the presence of *Diplodia
sapinea*

Matilda Stein Åslund



Independent project • 30 ECTS

Swedish University of Agricultural Sciences, SLU
Department of Forest Mycology and Plant Pathology
Uppsala 2020

A window to the future of Sweden's pine forestry? Development of declining Scots pine after a severe drought and the presence of *Diplodia sapinea*

Matilda Stein Åslund

Supervisor: Jan Stenlid, Swedish University of Agricultural Sciences, Department of Forest Mycology and Plant Pathology

Assistant supervisor: Laura Brodde, Swedish University of Agricultural Sciences, Department of Forest Mycology and Plant Pathology

Assistant supervisor: Malin Elfstrand, Swedish University of Agricultural Sciences, Department of Forest Mycology and Plant Pathology

Examiner: Karina Engelbrecht Clemmensen, Swedish University of Agricultural Sciences, Department of Forest Mycology and Plant Pathology

Credits: 30 ECTS

Level: Advanced level, A2E

Course title: Master Thesis in Biology

Course code: EX0895

Course coordinating dept: Department of Forest Mycology and Plant Pathology

Place of publication: Uppsala

Year of publication: 2020

Cover picture: Matilda Stein Åslund

Online publication: <https://stud.epsilon.slu.se>

Keywords: *Pinus sylvestris*, Scots pine, *Diplodia sapinea*, *Sphaeropsis sapinea*, *Diplodia pinea*, drought, climate change

Swedish University of Agricultural Sciences
Faculty of Natural Resources and Agricultural Sciences
Department of Forest Mycology and Plant Pathology

Publishing and archiving

Approved students' theses at SLU are published electronically. As a student, you have the copyright to your own work and need to approve the electronic publishing. If you check the box for **YES**, the full text (pdf file) and metadata will be visible and searchable online. If you check the box for **NO**, only the metadata and the abstract will be visible and searchable online. Nevertheless, when the document is uploaded it will still be archived as a digital file.

If you are more than one author you all need to agree on a decision. You can find more information about publishing and archiving here: <https://www.slu.se/en/subweb/library/publish-and-analyse/register-and-publish/agreement-for-publishing/>

YES, I/we hereby give permission to publish the present thesis in accordance with the SLU agreement regarding the transfer of the right to publish a work.

NO, I/we do not give permission to publish the present work. The work will still be archived and its metadata and abstract will be visible and searchable.

Abstract

Swedish forestry is dominated by uniform conifer stands, a structure generally more susceptible to biotic and abiotic stressors. Among the agents causing forest decline, pathogenic fungi have the most substantial impact. This thesis presents an example of a “disease triangle”; the interaction between Scots pine, the fungus *Diplodia sapinea*, and the environmental aspects affecting them.

Scots pine has low demands on nutrient and water supply and is a strong competitor in poor soils. *D. sapinea* causes *Diplodia* shoot blight, a common pine disease that can lead to severe damages. The fungus is particularly infectious when the weather is wet and warm, and when the trees experience stress.

The study focuses on Gotland, an island where *D. sapinea* was found in connection to a severe drought period in 2018. The aims were to identify drivers of and monitor the decline in Scots pine on four symptomatic and four asymptomatic sites on the island, by estimating defoliation levels, assessing *D. sapinea* spore release, and analysing the local climate at the sites during one year after the drought period, as well as testing correlations of the decline with soil properties.

Trees with a high level of defoliation just after the drought period experienced a larger increase in defoliation the following year than trees with initially low defoliation levels. Trees did generally not recover during the experimental period. The spore load was overall higher at symptomatic sites, but the difference between site types by season was only significant in summer. The spore load was positively correlated to precipitation and wind speed. Relative humidity was overall higher at asymptomatic sites, and asymptomatic sites experienced less extreme temperatures. The soil type differed between the site types, although soil analyses showed no significant differences between asymptomatic and symptomatic sites regarding nutrients, pH, loss on ignition and water-holding capacity.

Conclusively, this study shows that the decline in Scots pine related to *D. sapinea* is strongly driven by drought stress and that an inadequate site may be what enables a disease triangle to be complete.

Keywords: *Pinus sylvestris*, Scots pine, *Diplodia sapinea*, *Sphaeropsis sapinea*, *Diplodia pinea*, drought, climate change

Table of contents

1. Introduction.....	9
1.1. Forest diseases and the disease triangle.....	9
1.2. Host tree: <i>Pinus sylvestris</i>	10
1.2.1. <i>Pinus sylvestris</i> in Sweden	11
1.3. Pathogen: <i>Diplodia sapinea</i>	11
1.3.1. <i>Diplodia sapinea</i> in Sweden	14
1.4. Environment: Factors affecting the interaction between host (<i>Pinus sylvestris</i>) and pathogen (<i>Diplodia sapinea</i>).....	14
1.4.1. Soil nutrients and properties	14
1.4.2. Drought stress.....	17
1.4.3. Climate change	19
1.5. Case study on Gotland.....	20
1.6. Aims and hypotheses	20
2. Materials and methods.....	21
2.1. Experimental sites	21
2.2. Studied trees	22
2.2.1. Included individuals.....	22
2.2.2. Tree measurements.....	23
2.2.3. Damage estimation	23
2.2.4. Data analysis of studied trees.....	23
2.3. Spore loads	24
2.3.1. Spore traps	24
2.3.2. Quantification of <i>D. sapinea</i> spores using qPCR	25
2.3.3. Spore load data analysis	27
2.4. Climate.....	29
2.4.1. Climate data collection.....	29
2.4.2. Local climate data analysis.....	29
2.5. Soil properties.....	30
2.5.1. Soil type and soil depth.....	30
2.5.2. Soil nutrient and property analysis.....	30
3. Results.....	34

3.1.	Studied trees: Tree damage	34
3.2.	Spore loads	36
3.3.	Local climate.....	39
3.4.	Soil properties.....	45
3.4.1.	Soil type	45
3.4.2.	Soil depth	45
3.4.3.	Soil nutrients and properties	46
4.	Discussion.....	49
4.1.	The analyses	49
4.1.1.	Studied trees: Tree damage	49
4.1.2.	Spore loads.....	50
4.1.3.	Local climate	51
4.1.4.	Soil properties.....	51
4.1.5.	Conclusion results.....	52
4.2.	The outbreak of <i>D. sapinea</i> on Gotland	53
4.3.	Future	54
4.4.	Conclusion	55
	References	57
	Appendix	63
	Appendix 1.....	63
	Studied trees	63
	Appendix 2.....	65
	Soil nutrients and properties.....	65
	Soil properties – principal component analyses.....	66

1. Introduction

1.1. Forest diseases and the disease triangle

Swedish forestry is dominated by even-aged conifer stands. Stand uniformity entails low value for biodiversity and wildlife, and such stands are generally more susceptible to pathogens and pests, and more sensitive to global warming (Fridman, 2005). It is difficult to quantify the relative impact of the different factors contributing to forest decline (Gonthier, 2013), i.e., premature loss of vigour and health in forest trees (Sinclair and Hudler, 1988). The public, regulators, and policymakers often rank fire and insects first as destructive agents, but in reality, diseases cause the majority of timber losses, not only due to tree mortality but also by a reduction in growth and wood quality (Gonthier, 2013). Among the diverse range of organisms causing infectious diseases in forests, fungi constitute the largest group (Edmonds, 2013).

A forest disease epidemic can be conceptualised as the result of the interaction between a susceptible host plant, a virulent pathogen, and a, from the perspective of the disease, favourable environment, which can be visualised by the disease triangle (Fig. 1) (Agrios, 2005).

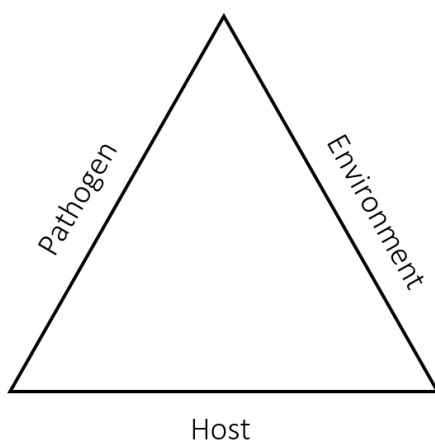


Figure 1. The disease triangle (Agrios, 2005).

A pathogen's ability to cause disease depends on its pathogenicity factors; virulence, type of inoculum, dispersal potential, inoculum potential (e.g., the energy carried by the pathogen at the point of infection), host range, and potential host alternation. The host factors influencing epidemics are tolerance and resistance, developmental stage (related to both age and season), and stand uniformity. Disease develops as the synchronisation of pathogen and host factors is affected by environmental factors, such as drought, frost, competition, or forest management (Oliva *et al.*, 2013).

An example of a disease triangle is the interaction between *Pinus sylvestris* (Scots pine), the fungus *Diplodia sapinea*, and the environmental aspects that disrupt the balance between the organisms.

1.2. Host tree: *Pinus sylvestris*

Scots pine (*Pinus sylvestris*) is the most widely distributed *Pinus* species in the world (Skilling, 1990). Its natural distribution ranges from Scotland to the Siberian taiga, and from the Mediterranean to beyond the Arctic Circle in Scandinavia (Skilling, 1990; Pyhäjärvi and Kujala, 2020), and it is encountered on altitudes from sea level to near 2500 m (Skilling, 1990). Compared to other *Pinus* species, it has a broad ecological niche (Pyhäjärvi and Kujala, 2020). It is a strong competitor in poor soils, with low demands on soil depth, nutrients, and water supply (Albrektsson *et al.*, 2012). It is also a strong competitor in dry and cold environments (Pyhäjärvi and Kujala, 2020), and as indicated by its large natural range, *P. sylvestris* is adapted to a variety of climates; growing in areas with reported annual precipitation from 200 mm to 1780 mm and in areas with winter temperatures recorded below -60°C, as well as in subtropical regions (Skilling, 1990). The tree grows on a wide variety of soil types from ancient rock to the most recent glacial deposits with various levels of podsolisation. It can even be found on peatland, although usually considerably stunted (Skilling, 1990).

P. sylvestris is a dominant tree in forests of the northern parts of its range. Here, it is of great importance for the forest ecosystems, mainly through its interaction with soil microbes and fungi, and for global carbon reservoirs. Beyond, Scots pine is of high economic importance, and it is cultivated for timber, raw paper material and pulp industry well outside of its natural distribution range. It is estimated that Scots pine cover over 145 million ha of forest in Eurasia. In terms of species viability, *P. sylvestris* is not under global threat, but any changes in its distribution or mortality would presumably have substantial consequences, both ecological and economic, due to its dominance in forest ecosystems (Pyhäjärvi and Kujala, 2020).

1.2.1. *Pinus sylvestris* in Sweden

Swedish forest owners are often recommended to plant Scots pine in forests that are dry, or that have a thin soil layer, sparse ground vegetation, and low water-holding capacity (Albrektsson *et al.*, 2012; Heurgren Film, 2019). Among the dominant tree species in Sweden, Scots pine has shown to be the least demanding and most tolerant in experiments on nutrition requirements (Ingestad, 1978).

In the latest five-year average estimation (2014-2019), Sweden had 22.3 million ha of productive forest, of which 8.8 million ha was pine (Swedish National Forest Inventory, 2019). 45% of the trees planted in Swedish forests 2019 were pine (172.5 million plants) (Swedish Forest Agency, 2020) and 34% (27.4 million m³) of the harvested volume was pine in the latest five-year average estimation (2014-2019) (Swedish National Forest Inventory, 2019).

1.3. Pathogen: *Diplodia sapinea*

One of the most common diseases in pines, and other conifers, is *Diplodia* shoot blight. It is caused by the ascomycete fungus *Diplodia sapinea* (Fr.) Fuckel (synonyms *Diplodia pinea* (Desm.) Kickx., *Sphaeropsis sapinea* (Fr.: Fr.) Dyko and Sutton, *Diplodia sapinea* will be used in this thesis, as suggested by Phillips *et al.*, 2013) (Stanosz *et al.*, 2001). The disease affects 33 species of pine (Palmer, 1987) and is present on all continents (Stanosz *et al.*, 2004; CABI, 2019) (see Fig. 2).



Figure 2. World map showing the distribution of *Diplodia sapinea* as of July 2020. Reported findings indicated by one orange dot per country/state/province. The map is retrieved from CABI (2020).

In natural forests, *D. sapinea* and other fungi responsible for branch and tip blights are mostly related to modest, scattered damage as a result of periods of stress events (Capretti *et al.*, 2013). In monoculture plantations in temperate forests, *D. sapinea* is widely distributed and causes severe damages, particularly on sites with high relative humidity during flushing and with mild summers. The present distribution of the fungus in forest ecosystems is greatly affected by human disturbance, increased monoculture management, planting of exotic tree species, and the intensified international trade of plant material facilitating the introduction of pathogens to new areas. Those factors have changed the behaviour of the fungus, from being a weak pathogen causing low levels of damage to become a very harmful one (Capretti *et al.*, 2013). In northern and central Europe and North America, Scots pine and Austrian pine (*Pinus nigra*) are among the most common species in reforestation. Reports from the late 1800s and early 1900s show that these species have enabled the spread and colonisation of fungal pathogens such as *D. sapinea* across the world (Capretti *et al.*, 2013).

Diplodia shoot blight can affect trees at all ages by weakening them over a long period or, sometimes, rapidly killing them during only one growing season (Stanosz *et al.*, 2004). *D. sapinea* spreads via windborne conidia, which are released in spring and summer (Capretti *et al.*, 2013). *D. sapinea* conidia are large for being spores, with a length of 30-45 μm , and a width of approximately 12 μm (Butin, 1989), a trait that is believed to reduce their ability to spread long distances (Norros *et al.*, 2014). They are brown and of a bean-like shape (see Fig. 3). *Diplodia ssp.* conidia and spores can be identified morphologically, but identification on species-level require molecular methods (Capretti *et al.*, 2013).

The fungus prefers host tissue high in nutrients (e.g., mesophyll, vascular cambium, medullary rays, phloem of weakened plants) (Capretti *et al.*, 2013) and penetrates elongating needles through stomata, or infects young, non-suberised stems or fresh wounds, during moist periods (Stanosz *et al.*, 2001). The onset of infection is favoured by rainy, hot weather (Capretti *et al.*, 2013), as well as mechanical wounds, drought, and other stress factors (Brodde *et al.*, 2019).

After entering the host, the fungus forms mycelia (intercellular or superficial) that absorb nutrients by penetrating the plant, leading to the meristem tissue dying (Capretti *et al.*, 2013). Pycnidia (asexual fruiting bodies) are produced in the tissue of green shoots and needles, and germinating conidia infect young tissue (see Fig. 3). Mycelia are developed in the infected tissue, and then colonise resin ducts, permeate cells and grow inter- and intracellularly in the tissue (Capretti *et al.*, 2013). Pycnidia form as small, black pustules on infected tissue in late summer (Fig. 3) (Capretti *et al.*, 2013). Sexual reproduction has not been observed in *D. sapinea* (Phillips *et al.*, 2013).

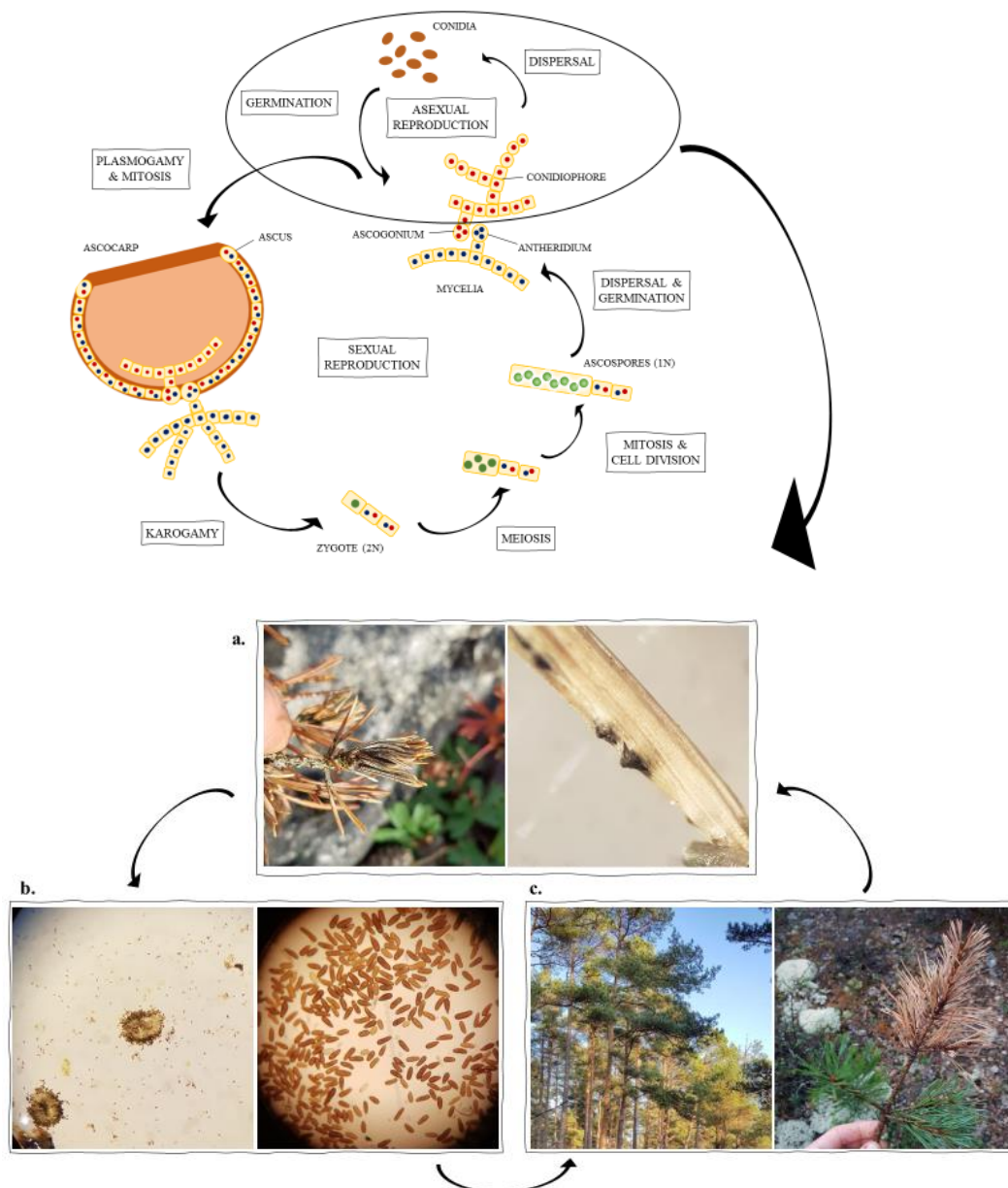


Figure 3. The Ascomycota life cycle and the asexual reproduction cycle of *D. sapinea*. a. Pycnidia are produced in and emerge from plant tissue. b. Pycnidia release conidia. c. Germinating conidia infect young tissue of trees. (Ascomycota life cycle modified from VectorMine.com, photos by M. Stein Åslund).

Symptoms are visible shortly after infection (Stanosz *et al.*, 2001). The symptoms are necrosis and chlorosis of whole needle or needle base, light brown or tan discolouration of needles, dry and twisted twigs and needles, shoot dieback and cankers with emerging pycnidia (Brookhouser and Peterson, 1971; Chou, 1976; Nicholls and Ostry, 1990). As the infection spreads in the tree, the crown becomes brownish/red (Capretti *et al.*, 2013).

Virulent isolates of the pathogen have been recovered from asymptomatic trees of several *Pinus* species as well as other conifers, proving that *D. sapinea* can act as a latent pathogen (Blodgett and Stanosz, 1999; Stanosz *et al.*, 2001). The fungus also survives as a saprophyte, and the inoculum can live for several years on infected cones or twigs lying on the ground (Capretti *et al.*, 2013). Thus, under optimal conditions, *D. sapinea* can act in an opportunistic manner and cause rapid disease development (Stanosz *et al.*, 2001; Capretti *et al.*, 2013).

D. sapinea can cause rot on seeds, collar rot on seedlings, damping off, cankers on stem and branches, staining of sapwood, and shoot blight (Stanosz *et al.*, 2004). The wood of infected pine trees gets darkened, and severe infection leads to the tree dying (Capretti *et al.*, 2013). *D. sapinea* is a highly economically destructive pathogen due to the killing of leader shoots, disruption of crown shape, and the overall decrease in stem quality (Chou, 1976; Zwolinski, Swart and Wingfield, 1990; Brodde *et al.*, 2019).

1.3.1. *Diplodia sapinea* in Sweden

D. sapinea is known to have been present in Swedish forest nurseries in the 1950s (Molin, Persson and Persson, 1961), but the pathogen was not reported in a Swedish forest until 2013 (Oliva, Boberg and Stenlid, 2013). The first large-scale outbreak on *P. sylvestris* in Sweden was discovered in 2016, when a 15 ha plantation in Arlanda, north of Stockholm, was found to be severely damaged by the pathogen (Brodde *et al.*, 2019). *D. sapinea* has since been recorded in many parts of Sweden, from Skåne in the south to Härjedalen in the north (Jan Stenlid, personal communication), and has recently been detected on the islands of Öland (unpublished data) and Gotland along the east coast.

1.4. Environment: Factors affecting the interaction between host (*Pinus sylvestris*) and pathogen (*Diplodia sapinea*)

1.4.1. Soil nutrients and properties

Although Scots pine grows well on various soils, optimum growth is achieved on well-drained sands and gravels, preferably on hills or terraces in the landscape (Skilling, 1990). *P. sylvestris* can grow on soils with a wide pH range but thrives at a pH ranging from 4.5-6.0 (Skilling, 1990). Regardless of its low demands, pines need water and essential elements for survival. Seventeen elements are essential for vascular plants; eight micronutrients (molybdenum, nickel, copper, zinc,

manganese, boron, iron and chlorine) and nine macronutrients (nitrogen, sulphur, magnesium, phosphorus, potassium, calcium, hydrogen, carbon and oxygen). Nitrogen, phosphorus and potassium are, in that order, the nutrients most likely to limit plant growth (Brady and Weil, 2008). However, Evert, Eichhorn and Raven (2004) claim that phosphorus is the element most likely limiting growth in plants.

Plant roots take up nitrogen mainly as nitrate and ammonium ions (Brady and Weil, 2008). A study on mineral nutrient requirements of *P. sylvestris* seedlings by Ingestad (1978) showed equal efficiency in growth with various ratios of ammonium and nitrate nitrogen, except for a growth reduction when seedlings were provided with nitrate only. Nitrogen is a fundamental part of all amino acids, meaning it is included in all enzymes, the nucleic acids, and chlorophyll (Evert, Eichhorn and Raven, 2004). Given its involvement in amino acids, some of which are secondary metabolites participating in plant defence, nitrogen availability is influencing plant-pathogen interactions (Sherwood *et al.*, 2015). A balanced supply of nitrogen stimulates growth and development of roots, nutrient uptake, and plant productivity (Evert, Eichhorn and Raven, 2004; Brady and Weil, 2008). Nitrogen deficiency leads to a low shoot-to-root ratio and negatively affects plant vigour. Oversupply, on the other hand, leads to excessive growth with enlarged but weak stems and top-heavy plants that risk falling over. High nitrogen levels can delay maturity in plants and thereby increase the susceptibility to insect pests and pathogens, especially to fungal pathogens (Brady and Weil, 2008).

Phosphorus constitutes an essential part of nucleic acids and biologically important redox couples. A balanced supply of phosphorus enhances photosynthesis, nitrogen fixation, seed production, and root growth. Whereas, deficiency of phosphorus can lead to stunted growth and thin stems (Brady and Weil, 2008).

Potassium plays a vital role in reducing water loss from leaf stomata and increasing root cell water uptake, by lowering cellular osmotic water potentials. Potassium helps plants adapt to environmental stresses, and it is associated with increased drought tolerance, higher resistance to fungal diseases, and improved tolerance to insect pests. Deficiency has the opposite effect; higher sensitivity to drought and other stressors, increased lodging, etc. (Brady and Weil, 2008).

Calcium is involved in cell elongation and division, and it controls stomatal opening and closing by regulating ionic gradients (Evert, Eichhorn and Raven, 2004). Deficiency shortens the roots, makes the root system denser, and has a negative effect on meristems (Brady and Weil, 2008). Excess calcium can lead to “lime-induced chlorosis” (Ingestad, 1978), commonly caused by disturbances in iron nutrition (Lindner and Harley, 1944), which can occur when high soil pH leads to iron becoming unavailable to plants (Pavloušek, 2010). However, Scots pine has

been shown to have high adaptability in the mechanism for calcium uptake. Even on lime-rich soils, pine needles have a low calcium content, making the tree species less prone to the chlorosis (Ingestad, 1978).

Magnesium is involved in photosynthesis, oil and protein synthesis, and activation of energy metabolism enzymes. It is also participating in catalysing several physiological processes. Magnesium deficiency in conifers can lead to underdeveloped growth (Brady and Weil, 2008).

Sulphur is included in many enzymes that regulate photosynthesis and nitrogen fixation. Deficiency leads to thin stems and petioles and slow growth (Brady and Weil, 2008). Release of plant-available sulphate depends mainly on microbial processes, so the supply fluctuates with changes in the environment (seasonal and even daily), leading to difficulties measuring the plant-available sulphur in soils (Brady and Weil, 2008).

In experiments on Scots pine seedlings, growth rate peaked in nutrient solutions with the N:P:K:Ca:Mg weight proportions 100:14:45:6:6 (Ingestad, 1978). The required concentration range of nitrogen and optimum concentration ranges of phosphorus, potassium, calcium and magnesium in nutrient solution are listed in Table 1 (Ingestad, 1978).

Table 1. Required concentration range of N and optimum concentration ranges of P, K⁺, Ca²⁺ and Mg²⁺ in nutrient solution for P. sylvestris (Ingestad, 1978).

Macronutrient	Concentration (mg/L)
Nitrogen	20-50
Phosphorus	2.8-7.0
Potassium	9.0-22.5
Calcium	1.2-3.0
Magnesium	1.2-3.0

Soil organic matter is not directly essential to trees, as the carbon needed by higher plants is derived from carbon dioxide and the nutrients come mostly from dissolved inorganic ions in the soil. Plants can complete their life cycle growing without humus, but organic matter has great indirect benefits on the soil properties. Humus influences the soil water retention by improving both rates of infiltration and water-holding capacity. It provides pH buffering, as humus colloids hold nutrient cations (K⁺, Ca²⁺, Mg²⁺, etc.). Organic matter also accelerates the mineralisation and provides storage for nitrogen, phosphorus, sulphur and micronutrients. Besides, it provides nutrients for the soil organisms (Brady and Weil, 2008).

Many theories have developed that attempt to explain the dynamics of secondary metabolites in plants. The carbon-nutrient balance hypothesis, assuming that

secondary metabolite concentrations in plants are dictated by the availability of resources in the environment, has been widely used in studies on plant defence (Hamilton, Arthur and Delucia, 2001). Hamilton, Arthur and Delucia (2001) reject the carbon-nutrient balance hypothesis and suggest that theories based on evolution and adaptation, like the optimal defence theory, are more robust and applicable for plant systems. The optimal defence theory focuses on three factors that constitute defence; the importance of the tissue to the plant, the advantage of defence, and attack probability. Dietze *et al.* (2014) propose that secondary metabolite dynamics in trees are determined not only by resource availability but by a functional trade-off. Since trees have a long lifespan, their risk of being exposed to periods of abiotic and biotic stress is high relative to other plants, and they may benefit from allocating their carbon investment to secondary metabolites rather than to primary metabolites. Trees need to weigh the trade-offs between growth, storage and defence, particularly when resources are limited due to environmental stress (Huang *et al.*, 2020).

1.4.2. Drought stress

The leaves of pines, like them of most conifers, are well-suited for growth under harsh conditions with scarce water supplies (Evert, Eichhorn and Raven, 2004). However, having leaves that function for several seasons can be disadvantageous, giving exposure to higher risks of damage by freezing, drought, and air pollutions than leaves of deciduous plants (Evert, Eichhorn and Raven, 2004). Therefore, diseases affecting the tree crown often have a more severe impact on conifers. Particularly, damage to buds and young shoots can reduce growth, weaken the tree, and make it more susceptible to other threats (Capretti *et al.*, 2013).

According to Sturrock *et al.* (2011), fungi causing cankers are prone to become epidemic and lead to considerable damage to trees that are weakened by stressors like heat or drought. The severity of *Diplodia* shoot blight has been associated with water stress consistently (Bachi and Peterson, 1985; Blodgett, Kruger and Stanosz, 1997a, 1997b; Paoletti, Danti and Strati, 2001), and higher temperatures have been linked to *Diplodia* shoot blight damage in several studies (Fabre *et al.*, 2011; Bosso *et al.*, 2017; Brodde *et al.*, 2019). In a study by Nicholls and Ostry (1990), cankers caused by *D. sapinea* occurred more frequently on trees exposed to environmental stressors, such as poor site conditions, drought, hail, snow and wounding by insects. Sherwood *et al.* (2015) found that water-stressed pine trees were more susceptible to *D. sapinea*, and their experiments resulted in almost twice as long lesions caused by *D. sapinea* in Austrian pines exposed to water deficiency. Stanosz *et al.* (2001) reported a significant role of water stress in the initiation of collar rot in *D. sapinea*-colonised but asymptomatic *Pinus resinosa* seedlings. They suggest that the fungus

can be released from its latency phase by physiological alteration through drought stress (Stanosz *et al.*, 2001).

Several alterations in metabolism occur in the plant before symptoms of water deficit are visible; photosynthesis is limited, allocation of carbon changes, nutrient uptake is altered, and the levels of inorganic ions, soluble sugars, and amino acids change (Shao *et al.*, 2008).

Plants experiencing drought stress generally also experience increased oxidative stress (Sherwood *et al.*, 2015). Oxidative stress causes production of reactive oxygen species (ROS) and free radicals, both highly reactive and damaging to vital components of cells. ROS are involved in the defensive signalling pathways and are often also produced when the plant is infected, during which it can be directly toxic to the pathogen (Sherwood *et al.*, 2015). Sherwood *et al.* (2015) found that *D. sapinea* inoculated Austrian pines had a lower content of the key ROS hydrogen peroxide (H₂O₂) in the shoots, regardless of the nitrogen or water supplied in the experiment. They suggest that removing the ROS can facilitate fungal infection and growth and improve pathogenicity since it disrupts the plant's defensive signalling. They reported that activity in *Diplodia* peroxidase and catalase increased when the fungus was exposed to H₂O₂, particularly catalase, and propose that *Diplodia* catalase is what enables the fungi to remove H₂O₂.

Another plant response commonly related to drought is solute accumulation, especially of the amino acid proline (Sherwood *et al.*, 2015). When studying *P. sylvestris* responses to water deficit, Sancho-Knapik *et al.* (2017) found that the content of terpenoids increased when stomata closed at moderate water stress, which preceded the accumulation of proline and shikimic acid at severe water deficit, as photosynthesis reached negligible levels. Proline regulates osmotic pressure, is a compatible solute, can help stabilise subcellular structures, protects enzymes, helps prevent the formation of hydroxyl radical, regulates cellular redox homeostasis (often disturbed during stress), and helps the plant recover by being a source of nitrogen and carbon (Sherwood *et al.*, 2015). Proline often also accumulates when a plant is exposed to biotic stress. In *Arabidopsis* and tobacco, the metabolism of proline is believed to be involved in innate immunity by triggering hypersensitive response (HR), a type of programmed cell death, but its role in defence in most other systems is unclear (Sherwood *et al.*, 2015). Programmed cell death, coupled with activities that mobilise nutrients away from the infection, is a plant defence strategy often successful against biotrophic pathogens (Sherwood *et al.*, 2015). However, this strategy is inefficient against necrotrophic pathogens, like *D. sapinea*, and is instead promoting their infection (Govrin and Levine, 2000; Hammond-Kosack and Rudd, 2008).

Several studies have shown associations between altered host nutrition in pines and damages by *D. sapinea*, especially higher concentrations of nitrogen (van Dijk *et al.*, 1990; de Kam *et al.*, 1991; Blodgett, Herms and Bonello, 2005). Nitrogen in excess can stimulate drought stress; it alters the water relations in conifers by increased shoot-to-root ratio and decreased root biomass (van Dijk *et al.*, 1990), and reduces the needle water potential (de Kam *et al.*, 1991). Nitrogen surplus may also induce disease development in *D. sapinea* as nutrients in excess are more available and directly stimulatory to pathogens than to the hosts (Stanosz *et al.*, 2004). Because pathogens consume free and protein-bound amino acids from the host plant to get their required nitrogen, the drought-triggered accumulation of amino acids and other substrates is thought to further contribute to the increased level of disease in drought-stressed trees (Sherwood *et al.*, 2015).

1.4.3. Climate change

Although the complexity of the interactions between hosts and pathogens make future impacts challenging to predict, some general forecasts can be made on the influence of climate change on forest pathology (Sturrock *et al.*, 2011). Changes in environmental conditions will influence host and pathogen as well as the interaction between them, leading to changes in the impact of the disease. Since abiotic factors affect host susceptibility to pathogens, as well as growth, reproduction, and infection of the pathogen, disease outbreaks will presumably be driven by the interaction between disease and abiotic stressors. Increased temperatures and changes in precipitation will both reduce and expand the distribution of many pathogens and tree species. The impact of tree pathogens as destructive disturbance agents will probably increase since they have a higher ability to adapt to new environmental conditions than their hosts. Pathogens that typically affect water-deficit stressed trees will most likely benefit from reduced precipitation. Altered incidence and severity of diseases are expected due to affected life cycles and biological synchronicity of many pathogens and trees (Sturrock *et al.*, 2011).

If the climate becomes warmer and drier, it is predicted that the impact by *D. sapinea* will increase. A warmer and wetter climate is more difficult to predict but expected not to change the impact of the fungus substantially (Sturrock *et al.*, 2011). Humidity favours both Scots pine and *D. sapinea* since it facilitates the growth of shoots and young needles of the pine, as well as fruiting bodies of the fungus. It also benefits the pathogen by enabling the release of spores and germination of conidia. Extreme temperatures slow down the growth of both tree and fungus. Sunlight favours the host, as it inhibits germination of fungal propagules while enhancing cuticle and wax growth in needles. Declining trees are particularly susceptible if they are light deprived or water-stressed (Capretti *et al.*, 2013). In a study by Brodde *et al.* (2019), *D. sapinea* build-up of inoculum showed to be

favoured by warm spring conditions, potentially causing a more considerable impact by the fungus in Sweden than in other places, since spring temperatures are steadily increasing in the country.

1.5. Case study on Gotland

Sweden, and particularly Gotland, experienced severe drought during the summer of 2018 (Swedish Meteorological and Hydrological Institute, 2020). From an ecological point of view, Gotland is different from the rest of the country due to its maritime climate, low precipitation during the vegetation period, calcareous bedrock, and thin soil (Lindroos, 2001). The soil on Gotland is Inceptisol, an order of young soils where the beginning of profile development is visible but the well-defined characteristics of profiles of more mature soils are absent (Brady and Weil, 2008). Productive forest constitutes 42% of the island's area (Lindroos, 2001) of which 72.5%, or 81 400 ha, is *P. sylvestris* (Swedish National Forest Inventory, 2019). In late summer 2018, a prominent decline of the pines on non-productive forest lands on Gotland appeared, and *D. sapinea* was detected shortly after. Therefore, Gotland was identified as an ideal location for a case study. An experiment was set up to investigate the disease development at four symptomatic sites and four asymptomatic sites. Those eight sites were used in this study.

1.6. Aims and hypotheses

The aims of this thesis are to identify potential drivers of and monitor the development in decline in Scots pine on Gotland by (i) estimating defoliation levels approximately one year after the severe drought period in 2018, (ii) assessing spore release during one year as a proxy for *D. sapinea* infection levels, (iii) analysing the local climate at symptomatic and asymptomatic sites, and (iv) testing correlations of the decline with soil properties.

I hypothesised that 1) trees with a lower level of defoliation are more likely to recover than trees with high defoliation levels, that 2) symptomatic sites show higher spore loads than asymptomatic sites and that it applies for all seasons, that 3) relative humidity is higher in asymptomatic sites than in symptomatic sites and that 4) soil properties such as soil type, pH, available macronutrients and water-holding capacity are better suited to the needs of Scots pine at asymptomatic sites than at symptomatic sites.

2. Materials and methods

2.1. Experimental sites

All experimental sites are located east and northeast of Visby (see Fig. 4) as it is one of the areas on Gotland where Scots pines were the most affected after the drought period in 2018. All sites were chosen based on tree height and stand density to make sure they provided enough mature trees for the study. The symptomatic sites were chosen based on the poor health status of the trees, and the asymptomatic sites were chosen with the aim of finding healthy stands as close to the symptomatic sites as possible. Photos showing examples of a symptomatic and an asymptomatic site are presented in Fig. 5 a+b. From each site, samples were taken from 1-3 randomly chosen trees and examined to confirm the presence (at symptomatic sites) or absence (at asymptomatic sites) of *D. sapinea*.

The symptomatic sites (Gotland 1-4) are shown on the map in Fig. 4 as yellow dots (G1-G4). The coordinates in the centre of site Gotland 1 are 57.63587, 18.36288, site Gotland 2 is located at 57.63289, 18.41557, site Gotland 3 is located at 57.67524, 18.46347 and site Gotland 4 is located at 57.66042, 18.44692 (coordinate reference system SWEREF99 TM). The asymptomatic sites (Control 1-4) are shown on the map in Fig. 4 as green dots (C1-C4). Coordinates for the centre of site Control 1 are 57.63544, 18.35548, site Control 2 is located at 57.67979, 18.44784, site Control 3 have the coordinates 57.63607, 18.46947 and site Control 4 is at 57.63154, 18.41107 (coordinate reference system SWEREF99 TM).

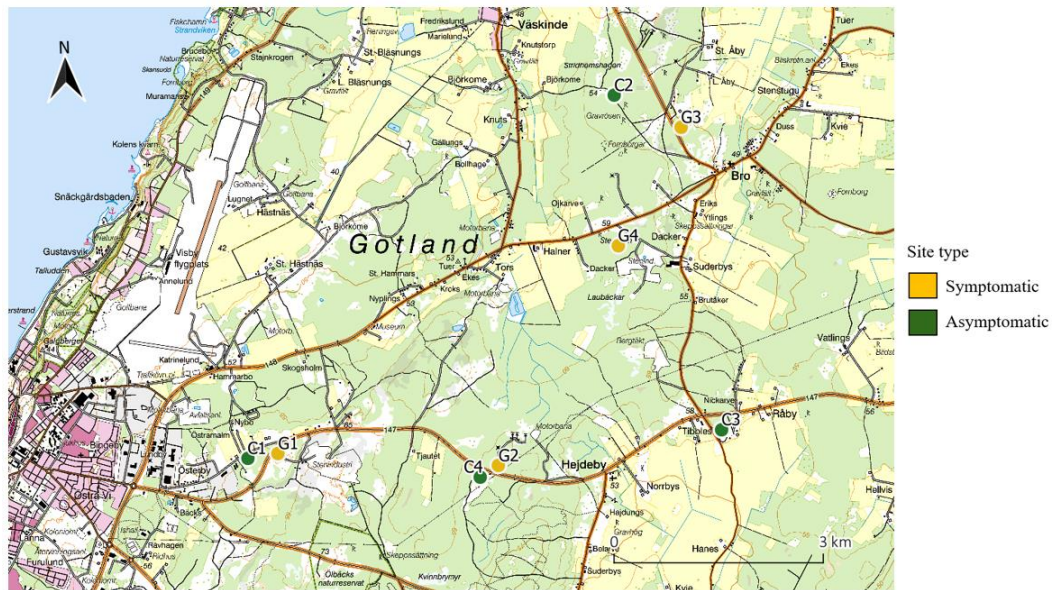


Figure 4. Map showing the location of the sites. Asymptomatic sites (C1-C4) indicated by green dots and symptomatic sites (G1-G4) indicated by yellow dots (GSD-Terrängkartan © Lantmäteriet, 2016).

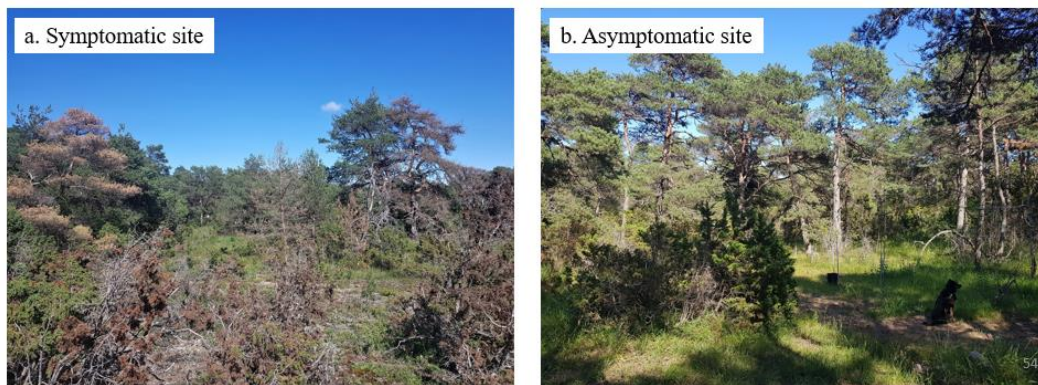


Figure 5. a+b. Photos from June 2019 showing examples of experimental sites. a: The symptomatic site Gotland 1 (G1). b: The asymptomatic site Control 1 (C1). (Photos by M. Stein Åslund).

2.2. Studied trees

2.2.1. Included individuals

The trees included in the study were selected in December 2018. The individuals at the symptomatic sites were chosen based on the level of defoliation of the crown, with the aim of including trees showing defoliation covering the span from almost no defoliation to almost completely defoliated.

There are 20 trees at site Gotland 1, 24 trees at Gotland 2, 25 trees at Gotland 3 and 27 trees at Gotland 4 included in the study. Within every asymptomatic site, five randomly selected trees are included. All trees in the study were given an ID number and labelled.

2.2.2. Tree measurements

For all trees included in the experiment at symptomatic sites, height was measured using a clinometer (Suunto, Vaanta, Finland) and diameter at breast height (DBH, 1.3 m) was converted from measurements of circumference using a measuring tape in December 2018. The same measurements were done for the trees at asymptomatic sites in May 2020.

2.2.3. Damage estimation

Defoliation level

Percentage defoliation of the upper third of the crown was estimated by visual examination for all trees included in the study in December 2018 and again in October 2019. The same person did both damage estimations. The estimation was limited to the upper third of the crown to avoid including the lower whorls where pine trees naturally self-shed the needles. Since the estimation was based on defoliation seen by eye, the percentage was not exact but categorised as 0 (no defoliation), 5, 10, 20, 30, 40, 50, 60, 70, 80, 90, and 100% (entire upper third of the crown defoliated).

Bifurcation

Bifurcation, the occurrence of several treetops due to disruption of the apical dominance in the leader shoot, was scored as present (1) or absent (0) for all trees included in the experiment.

2.2.4. Data analysis of studied trees

For the data analyses, the defoliation level in 2019 was converted to percentage defoliation of the residual crown according to equation 1;

$$\% \text{ defoliation residual crown} = \frac{\% \text{ defoliation 2019} - \% \text{ defoliation 2018}}{1 - \% \text{ defoliation 2018}} \quad (1)$$

A linear mixed-effects model was used to explain the relationship between defoliation of the residual crown in 2019 and the level of defoliation in 2018, presence of bifurcation, tree size, and total as well as seasonal spore load at the site.

Site identity was used as a random factor to account for variability within each site. Backwards selection was performed for model optimisation. Since tree height and diameter breast height are strongly correlated, only tree height was included in the model. Total spore load, as well as spore load for each spore trap period, were tested one at a time due to dependency. Total spore load showed a higher correlation with the defoliation in 2019 than any of the seasonal spore loads, and it was thereby used in the final model. (Methods to obtain spore load are described in section 2.3.).

2.3. Spore loads

2.3.1. Spore traps

To study the *D. sapinea* spore release, four spore traps were placed in the centre of each site. The traps consisted of one horizontally fixed filter paper (Munktell, Ahlström; 90 mm diameter) treated with 4x TE buffer, at the height of 1.2-1.5 m. The traps were up for seven days at a time, during two following periods per season with a total of eight sets during the year 2019; winter week 1 (January 22-January 29), winter week 2 (January 29-February 5), spring week 1 (April 10-April 17), spring week 2 (April 17-April 24), summer week 1 (July 15-July 22), summer week 2 (July 22-July 29), autumn week 1 (October 14-October 21), and autumn week 2 (October 21-October 28). The filter papers were collected in 50 mL Falcon tubes and kept cool during transportation to storage at -20°C. In this study, all spore traps from symptomatic sites were analysed except from spring week 2 (April 17-April 24), whereas for the asymptomatic sites, only spore traps from the first week of each season (January 22-29, April 10-17, July 15-22, and October 14-21) were analysed. One filter disappeared during a trapping period, presumably due to wind, and one was dropped on the ground and therefore discarded. A total of 174 spore trap filters were analysed.

DNA extractions spore traps

To wash the spores off the filter papers, 20 mL SDS buffer (0.05M Tris pH 8, 0.05M EDTA pH 8, 0.104M SDS, 1M NaCl, dissolved by incubation at 60°C for two days) was added to the Falcon tubes before they were incubated at 65°C for 90 mins and thereafter vortexed. The filter papers were then removed, and 20 mL 2-propanol was added to the SDS buffer. The samples were mixed thoroughly and incubated at RT (room temperature) overnight. The following day, the samples were centrifuged at 7000 rpm for 10 mins at RT before the supernatant was removed and the pellet was resuspended in 700 µL lysis buffer PL2 (Macherey-Nagel, Düren, Germany), and transferred to 2 mL screw-cap tubes containing ~130 mg 0.2 mm glass beads,

~200 mg 0.4 mm glass beads, ~200 mg 3 mm glass beads and ~4 mg diatomaceous earth (powdered siliceous sedimentary rock). The samples were lysed for 30 s at 5000 rpm using Precellys® 24 Tissue homogenizer (Bertin Instruments). Extractions were then performed using Macherey-Nagel NucleoSpin Plant II kit (Macherey-Nagel, Düren, Germany) according to the manufacturer's protocol, with increased volumes of buffer PL3 and buffer PC proportionally to the volume of lysis buffer PL2 used for resuspension of the pellet (2.33× the specified volume).

2.3.2. Quantification of *D. sapinea* spores using qPCR

Standard dilutions

To produce stock concentrations for qPCR standard dilutions, a *D. sapinea* isolate was used. Four replicates of the DNA template were amplified using PCR, with two non-template controls (nuclease-free water). The PCR reaction mix consisted of Green PCR Master Mix (Thermo Fisher Scientific) and 200 nM of each primer (forward GTAAAACTGACGTTGAGGGACG, reverse CATAATTGTCTGCCCGGACTACT, both corresponding to regions of AF051536, the small subunit of ribosomal RNA gene of one of the *D. sapinea* morphotypes) (Luchi *et al.* (2005)). Each reaction contained 25 µL reaction mix and 25 µL template. The PCR program was 5 min at 95°C, 35 cycles of 30 s at 95°C, 30 s at 50°C and 15 s at 72°C, followed by 5 min at 72°C.

The PCR product was analysed using gel electrophoresis. SB buffer was used in a 1.5% agarose gel with GelGreen® Nucleic Acid Gel Stain (Biotium) as fluorescent stain. 3 µL of each PCR product was analysed in the electrophoresis, and the Gene Ruler™ DNA ladder (Thermo Fisher Scientific) was used for sizing of the DNA. The electrophoresis was run for 25 minutes at 150 V. The gel was thereafter examined in UV-light to confirm that the desired product, with a fragment length of 79 bp (Luchi *et al.*, 2005), was amplified.

DNA from the remaining PCR product was precipitated as follows: 0.10× the volume of sodium acetate (3M) and 2.5× the volume of EtOH (95%, RT) were added. The samples were vortexed and incubated on ice for 30 mins, and then centrifuged at RT at max speed for 10 mins. The supernatant was discarded, and the pellets were washed twice by adding ~60 µL EtOH (70%, RT) and centrifuging for 3 mins at RT at max speed before removing the EtOH. The tubes were left open at RT to let the remaining EtOH evaporate, and the pellets were then resuspended in 50 µL nuclease-free water.

The DNA in the precipitated PCR product was quantified using Invitrogen Qubit 4 Fluorometer (Thermo Fisher Scientific) following the manufacturer's protocol for

the Qubit dsDNA HS Assay Kit. Based on the results of the quantification of DNA in the purified PCR product, the replicate with the highest concentration was used for dilutions from stock concentration of 1×10^6 copies per μL calculated using the Thermo Fisher DNA Copy Number and Dilution Calculator (Thermo Fisher Scientific). Serial dilutions in nuclease-free water were made down to 1×10^2 copies per μL .

qPCR reaction mix and protocol

The qPCR reaction mix was made according to Luchi *et al.* (2005) with modifications; 1x SsoAdvancedTM Universal Probes Supermix (BioRad), 250 nM each of forward (GTAAAAACTGACGTTGAGGGACG) and reverse (CATAATTGTCTGCCCGGACTACT) primer and 200 nM probe (AGGCTCGGGTAGCGAATAGGATTAGATACCC, an internal probe hybridising within the region amplified by the PCR primers to distinguish both *D. sapinea* morphotypes). Primers and probe were designed according to Luchi *et al.* (2005). Reactions were set up in duplicate, including the standard curve from 1×10^6 to 1×10^2 copies per μL and the non-template controls (nuclease-free water). In each well of the PCR plate, 15 μL of the reaction mix and 5 μL template were loaded. The qPCR program was 2 min at 95°C followed by 40 cycles of 10 s at 95°C and 15 s at 60°C.

Test qPCR

To estimate suitable dilutions of DNA template for the analyses using qPCR, a test run was performed. Ten samples were tested in four different dilutions with nuclease-free water; undiluted, diluted 1:1, diluted 1:4 and diluted 1:9. The reaction mix composition and qPCR protocol were as described in the section “*qPCR reaction mix and protocol*”. Based on the qPCR C_T values for the different dilutions of the samples, I decided to continue the analyses with the spore trap samples diluted 1:1 in nuclease-free water, since this dilution appeared to reduce the inhibition in undiluted samples but remain a concentration detectable by the qPCR.

qPCR

All samples were analysed using qPCR with the same reaction mix composition and protocol as described in the section “*qPCR reaction mix and protocol*”, with the exception of the number of replicates per template: The first three plates were run with DNA template and non-template controls in duplicates, but the procedure had to be repeated for numerous samples due to unstable measurements resulting in high standard deviations (presumably caused by difficulties measuring

concentrations close to the detection limit). The four remaining plates were run with the DNA template and non-template controls in triplicates.

qPCR data analysis

iQTM5 Optical System software (BioRad) was used to analyse the qPCR data. Samples showing abnormal amplification curves were excluded, and the baseline in the amplification curve was adjusted to be located just above the background noise of the first couple of cycles.

All samples with a C_T standard deviation >0.5 were excluded from further analysis. In runs where triplicates of each template were used, samples with a standard deviation >0.5 were examined for a potential outlier. A maximum of one replicate per template was deleted, and the sample was included in the analysis if the remaining replicates had a standard deviation <0.5. Samples were also excluded if their mean C_T value was >37.00 cycles, or if their mean C_T value was <3.00 cycles below the C_T value for any of the non-template controls. After excluding samples that were useless or not reliable, 159 samples remained for the statistical analyses.

2.3.3. Spore load data analysis

Data from a previous study by Brodde *et al.* (2019) was used to convert the copy number starting quantity obtained by qPCR to number of spores. The spore traps in their study consisted of both a microscopy slide (13×110 mm) covered with two stripes of tape coated with permanent adhesive on both sides and a filter paper (90 mm diameter). The method enabled manually counting spores on the microscopy slide as well as quantifying DNA from spores from the filter paper using qPCR. Their data included samples from one wet trap period (seven days, 24.4 mm precipitation in total) and one dry trap period (seven days, 3.6 mm precipitation in total). To estimate how many copies that represent one spore, the area of the filter paper analysed (1/50 of the total area since 1 µL out of 50 µL eluted DNA was analysed) relative to the area of the microscopy slide analysed (spores on 1/2 of the total area was counted) was calculated to get a factor which then was multiplied with their qPCR starting quantity copy number data (see Equation 2).

$$\frac{\frac{\text{Area filter paper}}{50}}{\frac{\text{Area microscopy slide}}{2}} \rightarrow \frac{\frac{63.6}{50}}{\frac{14.3}{2}} \rightarrow \frac{1.272}{7.15} = 0.178 \quad (2)$$

Linear regression was done on counted spores versus the adjusted starting quantity values on all their samples, as well as the wet spore trap period and the dry spore trap period separately, giving the equation $y = 513.73x + 17256$ ($R^2 = 0.248$) when

both periods were included, $y = 732.4x + 15859$ ($R^2 = 0.4329$) for the dry period, and $y = 355.83x + 17860$ ($R^2 = 0.1366$) for the wet period. Since the dry period (732 copies per spore) had the highest correlation between spores quantified using qPCR and manually counted spores, it was used for converting starting quantity copy numbers to spores in this study.

I eluted 100 μL of DNA from each filter paper, diluted it 1:1 and analysed 5 μL (1/40 of the total filter paper area), so the starting quantity values (SQ) were converted to spores by Equation 3.

$$\text{Number of spores} = \frac{SQ}{732} \times 40 \quad (3)$$

Regression analysis was used to explain the variance in the number of spores detected between the site types (symptomatic or asymptomatic) and between seasons. Due to overdispersion in the spore load count data, a negative binomial generalised linear model was used. Spore traps from the first week of every season from all eight sites were included in the model. Estimated marginal means were computed to inspect the relationship between different seasons.

To analyse if weather conditions affected the spore load, a generalised linear mixed model was used as it allowed incorporating a random factor to account for variability within each site, and handles non-normal distributed count data. To achieve the latter, Poisson distribution with a logarithmic link was selected. All analysed spore trap periods from symptomatic sites were included. The spore load was converted to integers in the model. Precipitation, temperature and wind were included in the full model, but temperature was excluded by backwards selection. (Regional climate data collection is described in section 2.4.2.).

After observation in the field, the efficiency of the spore traps in regard to the height of the trees was questioned. The correlation between spore load and mean tree height per site was analysed using a generalised linear model with Poisson family distribution. Spore load at all sites during the first week of each season were included in the model, with number of spores as integers.

R Studio version 1.1.463 (R Core Team, 2018) was used to perform the statistical analyses and create the graphs.

2.4. Climate

2.4.1. Climate data collection

Local climate data

Temperature and relative humidity were measured at each site every 20 minutes, from December 3, 2018, to October 24, 2019, using Tinytag Plus 2 TGP-4500 loggers (Gemini DataLoggers UK Ltd, Chichester, West Sussex, UK). Each logger was placed in a tree near the centre of the site, at an approximate height of 1.5-2.0 m and inside a plastic box facing upside down to protect it from weathering.

Regional climate data

Data for precipitation, temperature and wind speed during the spore trap periods were retrieved from SMHI (2020). The raw data consisted of daily data for accumulated precipitation from two weather stations (Visby airport and Visby D), temperature data from three measurements per day at Visby airport, and the mean wind during 10 mins, measured once per hour, at Visby airport. The mean accumulated precipitation per day from the two stations was used to calculate the accumulated precipitation for each spore trap period. The mean temperature from all measurements during each spore trap period was used, as well as the mean wind speed during each period. The regional climate data were analysed in relation to spore load, see section 2.3.3.

2.4.2. Local climate data analysis

The Tinytag logger data for temperature and relative humidity at each site were downloaded using EasyView Pro (Intab). Due to accidental overwriting of files, site Gotland 4 is missing data from June 26, 2019, to October 24, 2019, and the site was therefore excluded from July-October in the analyses.

The loggers recorded peaks and drops of relative humidity (>100% and <0%), probably due to malfunction, and those measurements were deleted as suggested by the manufacturer. Daily average, maximum and minimum values were extracted for temperature and relative humidity at each site. The data were detrended to get rid of noise with a three-day window (giving the value for day 2 as the average of day 1-3). From the daily data for temperature and relative humidity, mean, maximum and minimum values were extracted for each month.

To test whether the site condition (symptomatic or asymptomatic) was related to mean, minimum and maximum temperature and relative humidity, a generalised

linear model was used with binomial distribution. Temperature and relative humidity were tested separately due to lack of independence.

Estimated marginal means on a linear model were computed to investigate the relationship between the relative humidity per month and site type, and between temperature per month and site type.

R Studio version 1.1.463 (R Core Team, 2018) was used to perform the statistical analyses and create the graphs.

2.5. Soil properties

2.5.1. Soil type and soil depth

Soil type (raster 10×10 m) and soil depth (raster 10×10 m) at each site was obtained from Geological Survey of Sweden (SGU, 2014, 2017) and analysed using QGIS (QGIS Development Team, 2019). The soil type data is compiled based on historical, manually drawn soil type maps (SGU, 2014). The soil depth data is based on interpolation from drilling surveys, mapping, and point observations (SGU, 2017).

2.5.2. Soil nutrient and property analysis

Soil sampling

Soil sampling was conducted at all eight sites in order to analyse pH, water-holding capacity, loss on ignition (to estimate organic content), and plant available ammonium, nitrate, potassium, calcium and phosphorus. At the asymptomatic sites, soil underneath all five studied trees was sampled. At the symptomatic sites, soil underneath the five most healthy (least % defoliation) and the five most affected (most % defoliation) trees were sampled. A total of 60 trees were sampled. For each tree, two soil cores were collected using a soil corer (3.0 cm diameter). The cores were taken on opposite sides of the tree, north and south (located using a compass), approximately halfway between the stem and the outer edge of the crown. A maximum of five tries per core was set with the aim of getting one solid core. All five trial cores per side were taken within the northern quarter or the southern quarter of the area around the tree, still with the same distance from the stem. When hitting bedrock or roots, the corer was moved to the right for a new try, then to the left, then further to the right than the previous try, etc. (see Fig. 6).

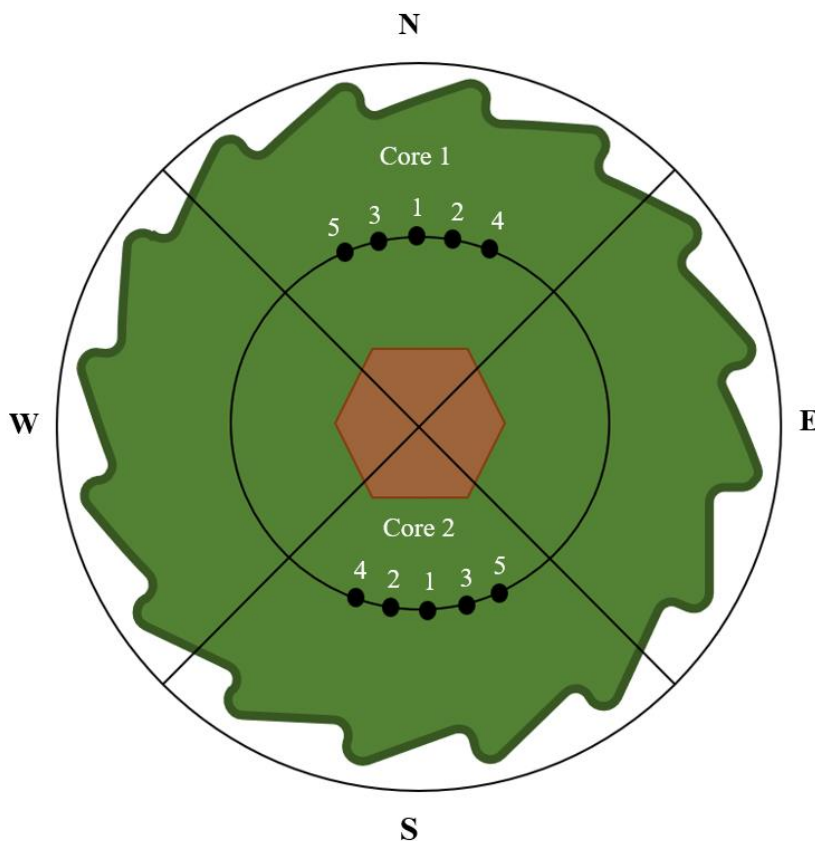


Figure 6. Illustration of tree crown as seen from above, showing the method for soil sampling underneath the tree. Two soil cores, taken on the north and the south side respectively, were collected from the ground approximately halfway between the stem and the outer edge of the crown of each tree. A maximum of five tries was set (indicated by black dots) to get one solid core per side. When hitting bedrock or roots, the corer was moved to the right for a new try (try 2), then to the left (try 3), then further to the right than the previous try (try 4), then further to the left again (try 5).

The two cores from each tree were divided into humus layer, centre layer (where humus and mineral were mixed) and mineral layer by cutting the core with a knife on a plastic cutting board, and the layers from the two cores were pooled in the same plastic bag, marked and kept cool during transport to storage at -20°C . The corer, knife and cutting board were cleaned with EtOH (70%) between groups of samples and between sites.

Soil analysis

Due to the small amount of soil sampled, the humus and centre layers for each tree were pooled for analysis. pH was measured on the pooled sample for each tree. For the remaining analyses, the soil samples were pooled per group (soil from asymptomatic sites – group CH, soil from healthy trees at symptomatic sites – group GH, soil from affected trees at symptomatic sites – group GA). Given that several samples lacked a mineral layer, mineral soil was excluded from the analyses in

order to obtain comparable results. The Soil and Plant Laboratory at the Department of Soil and Environment (Swedish University of Agricultural Sciences) performed all laboratory analyses of the soil.

pH was measured by air drying and sieving each sample (<2 mm), before a representative subsample was weighed in a 50 mL plastic tube. 25 mL de-ionised water was added, and the tube was shaken to suspend the soil in the water. The suspension sat overnight, and the pH was measured with a glass electrode the following day (Swedish University of Agricultural Sciences, 2020b).

Water-holding capacity (mL H₂O/100 g dry soil) was determined with a method modified from (Harding and Ross, 1964); a subsample from each soil sample was placed in a pre-weighed glass funnel. The funnel was plugged with glass wool to retain the soil and a rubber stopper at the end, filled with water and covered with a watch glass overnight. The following day, the rubber stopper was removed, and water was drained from the funnel for 8 hrs before the samples were dried in 105°C for 24 hrs.

Loss on ignition was analysed by drying subsamples of the soil samples at 105°C overnight to remove excess water. The following day, each sample was weighed, dried at 550°C for 4 hrs and weighed again to obtain the loss on ignition (Swedish University of Agricultural Sciences, 2020a).

To determine the NH₄⁺-N and NO₃⁻-N content in the soil samples, a method modified after Lindén (1981) and Lindén (2013) was used: Each sample was freeze milled (<10 mm) and stored at -18°C until extraction. 40 g of frozen soil was weighed in a plastic bottle, 100 mL 2M KCl solution was added, and the sample was placed in an end-over-end shaker at 15 rpm overnight. The next day, the extract was transferred to a centrifuge tube and centrifuged using a Rotixa 120 RS centrifuge for 10 min at 3000 rpm, before 10 mL of the extract was filtered through PALL Acrodisc PSF 10 µm syringe filters. The concentrations of NH₄⁺-N and NO₃⁻-N in the filtered extracts were determined using automated colourimetry (Seal, AutoAnalyzer 3). The water content in the soil samples was determined by drying a subsample of each sample in 105°C and the concentrations of NH₄⁺-N and NO₃⁻-N were reported on a dry weight basis.

P, K and Ca contents were determined using a method modified after the Swedish standard SS28310: The soil was dried in 35-40°C and sieved <2 mm, and 3 g of soil sample per element analysis was weighed into plastic tubes. 60 mL of ammonium lactate/acetic acid solution (AL-solution) was added to each sample before they were placed horizontally on the IKA HS 501 horizontal shaker, shaken for 90 minutes and filtrated through filter paper OOH (Munktell, Ahlström). The

final concentration of P, K and Ca (mg/100 dry soil) in the samples were determined using ICP/OES (Avio200, Perkin Elmer, USA).

Soil property data analysis

Correlation between the soil pH, water-holding capacity, loss on ignition, ammonium, nitrate, potassium, calcium and phosphorus was tested using a linear model. Due to correlation between several of them, all soil properties were analysed separately using a generalised linear model with binomial distribution to test if they explained site condition (symptomatic site = 1, asymptomatic site = 0) or group condition (affected trees at symptomatic sites (group GA) = 1, healthy trees at symptomatic sites (group GH) = 0, trees at asymptomatic sites (group CH) = 0). Estimated marginal means on a linear mixed-effects model were computed to investigate potential differences in soil properties between the group types (CH – asymptomatic sites, asymptomatic trees; GA – symptomatic sites, symptomatic trees; GH – symptomatic sites, asymptomatic trees).

R Studio version 1.1.463 (R Core Team, 2018) was used to perform the statistical analyses and create the graphs.

3. Results

3.1. Studied trees: Tree damage

The defoliation of the residual upper third of the tree crown at symptomatic sites in 2019 was correlated to the level of defoliation in 2018 (linear mixed-effects model; estimate = 0.324, SE = 0.124, df = 91, $t = 2.627$, $P = 0.010$ *) but not to the total spore load at the site (estimate = -0.002, SE = 0.001, df = 2, $t = -2.186$, $P = 0.160$), bifurcation, or tree size (represented by tree height). Contrary to the hypothesis, trees with a low percentage of defoliation of the upper third of the crown in 2018 were not more likely to recover between the years than trees with a high level of defoliation in 2018 (see Fig. 7). Data for defoliation in 2018 and 2019, tree height, diameter breast height and presence of bifurcation are presented in Appendix 1.

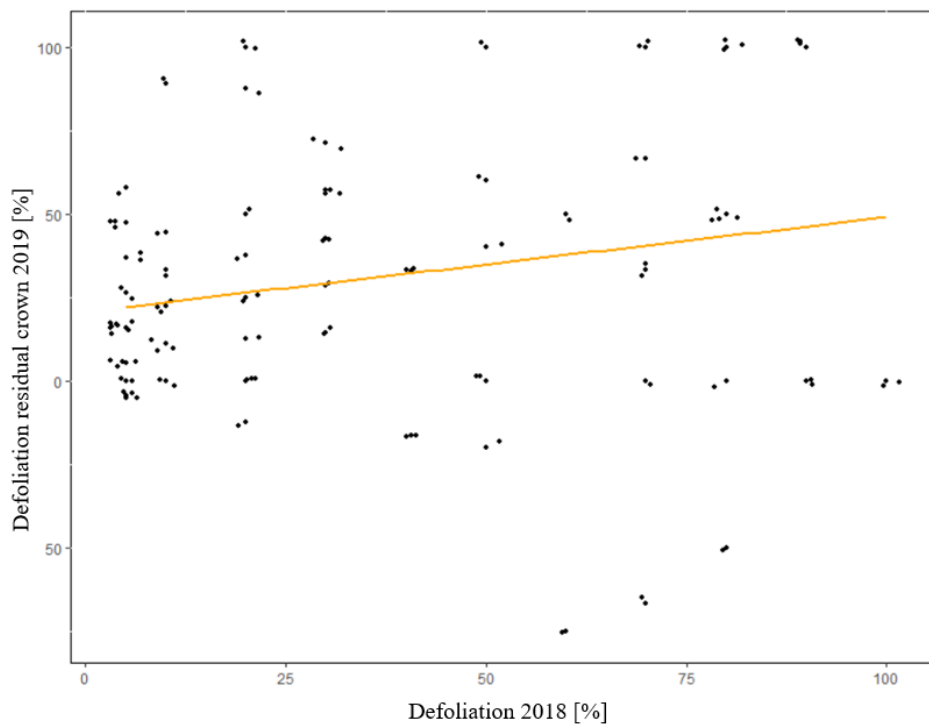


Figure 7. The effect of level of defoliation in 2018 (%) on defoliation of residual crown in 2019 (% defoliation of crown that was unaffected in 2018). The black dots show the tree individuals, and the yellow line shows the linear regression. Defoliation of residual crown in 2019 depends on the defoliation in 2018 ($P = 0.010$ *).

Defoliation levels of the residual crown in 2019 are visualised for all trees included in the study at all eight sites in Fig. 8. None of the trees at the asymptomatic sites (C1-C4) displayed defoliation in the first damage estimation in 2018, but when damage estimation was performed the second year, defoliation of up to 10% of the upper third of the crown occurred on trees at all four sites. C3 had the highest defoliation levels among the asymptomatic sites, with up to 20%. Defoliation of the entire crown (100%) occurred at all symptomatic sites in 2019. Site G1 and G2 had more trees with a substantial increase in defoliation than site G3 and G4. G3 was the site with most trees (five individuals) showing a lower level of defoliation in 2019 than in 2018, with up to 75% recovery of defoliation between the years (see Fig. 8).

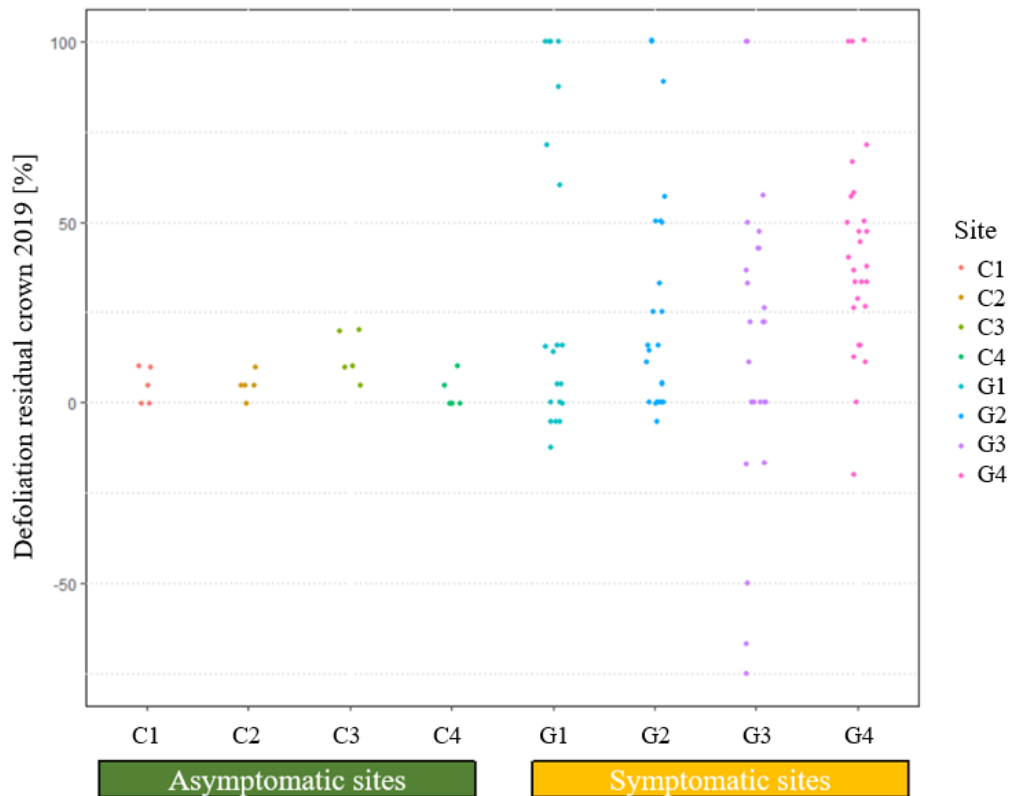


Figure 8. Percentage defoliation of residual crown in 2019 (% defoliation of crown that was unaffected in 2018) per tree at all sites (C1-C4 – asymptomatic sites, G1-G4 – symptomatic sites). The trees at asymptomatic sites were free from defoliation in 2018, but low levels of defoliation were displayed in individual trees at all four sites in 2019. Defoliation of the entire crown (100%) occurred at all symptomatic sites in 2019. Site G3 (purple dots) is the site with the most individual trees displaying less defoliation in 2019 than in 2018. In general, few trees recovered between the years.

3.2. Spore loads

The number of spores quantified from the first week of spore trapping for each season was overall higher in spore traps from symptomatic sites than in spore traps from asymptomatic sites (negative binomial generalised linear model; estimate = 1.395, SE = 0.418, z-value = 3.337, $P < 0.001$ ***) (see Fig. 9)). The difference between site types by season was only significant during the summer (see Table 2, Fig. 9).

Table 2. Estimated marginal means on the negative binomial generalised linear mixed model testing the difference in spore loads between symptomatic sites and asymptomatic sites by season.

Season	Estimate (asymptomatic sites)	SE	z-value ^a	P-value ^b	df ^c	Theta ^d
Winter	-1.10	0.865	-1.270	0.2041		
Spring	0.00	11000.0	0.000	1.000	Inf	0.896
Summer	-2.87	0.877	-3.270	0.0011 **		
Autumn	-1.79	1.310	-1.364	0.1724		

^a Estimate/SE

^b Significant P-values indicated by asterisks (***) $< 0.001 < ** < 0.01 < * < 0.05 < . < 0.1$

^c Degrees of freedom for overall model

^d Shape parameter of distribution for overall model

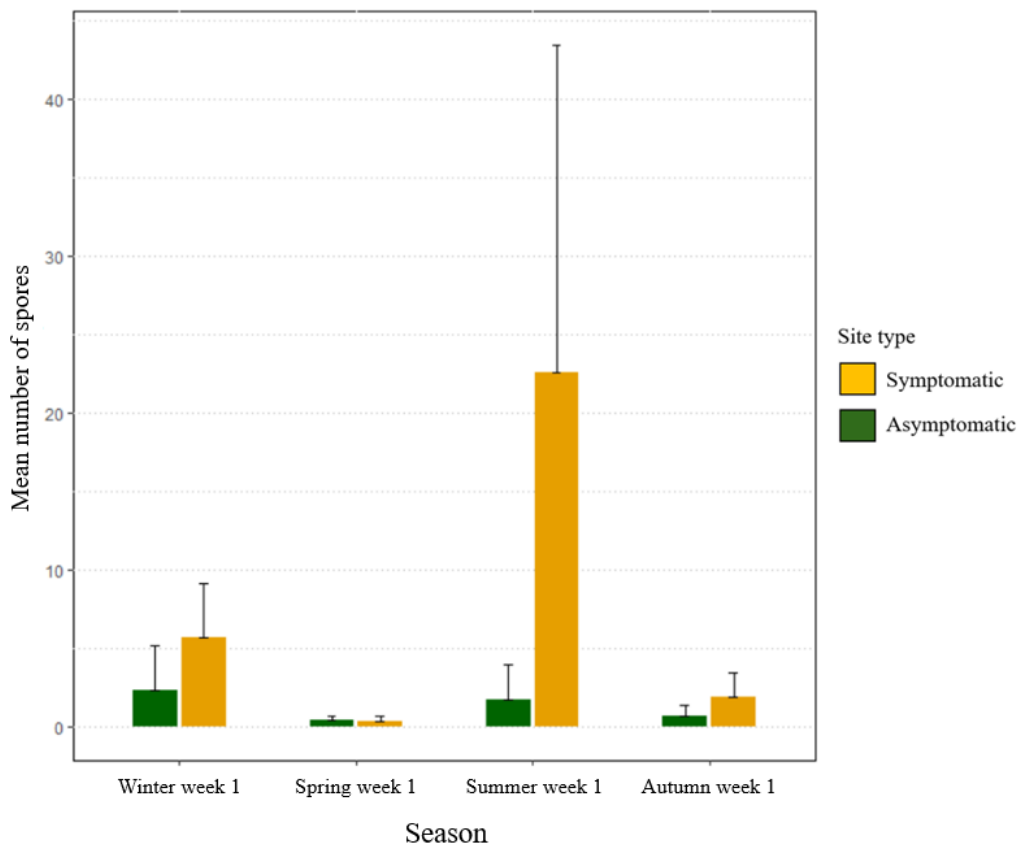


Figure 9. Mean number of spores quantified per site type (C – asymptomatic sites (green bars), G – symptomatic sites (yellow bars)) and season. Standard deviations indicated by black error bars. Only the first week of spore trapping per season is included. The number of spores is higher at symptomatic sites than at asymptomatic sites overall ($P < 0.001$ ***). The by season difference between the site types is only significant during the summer ($P = 0.001$ **). See also Table 2.

The analysis on whether the weather conditions during the spore trap periods affected the spore load at symptomatic sites showed correlations between spore load and wind speed, and between spore load and accumulated precipitation. The mean number of spores were positively correlated to mean wind speed (estimate =

0.140, SE = 0.041, z-value = 3.381, $P < 0.001$ ***) and accumulated precipitation during the week (estimate = 0.101, SE = 0.008, z-value = 12.165, $P < 0.001$ ***) (Poisson generalised linear mixed model). The average temperature did not have a significant effect on the spore load (see Fig. 10).

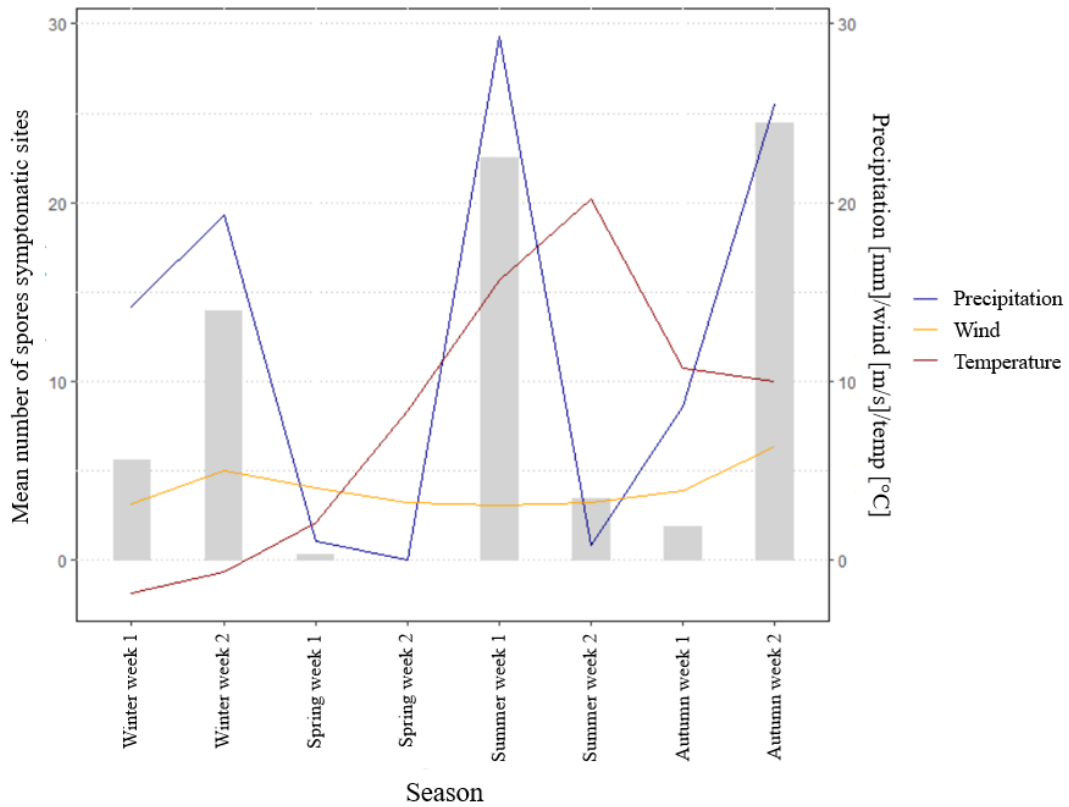


Figure 10. Mean number of spores detected at symptomatic sites (grey bars) and accumulated precipitation [mm] (blue line), mean wind speed [m/s] (yellow line) and average temperature [°C] (red line) during the spore trap periods. Spore load for the second week of spring is not analysed. Spore load is positively correlated to precipitation and wind speed ($P < 0.001$ ***)).

The variability in spore loads between sites was positively correlated to mean tree height at the sites (negative binomial generalised linear model; estimate = 0.505, SE = 0.218, z-value = 2.320, $P = 0.020$ * (see Fig. 11)).

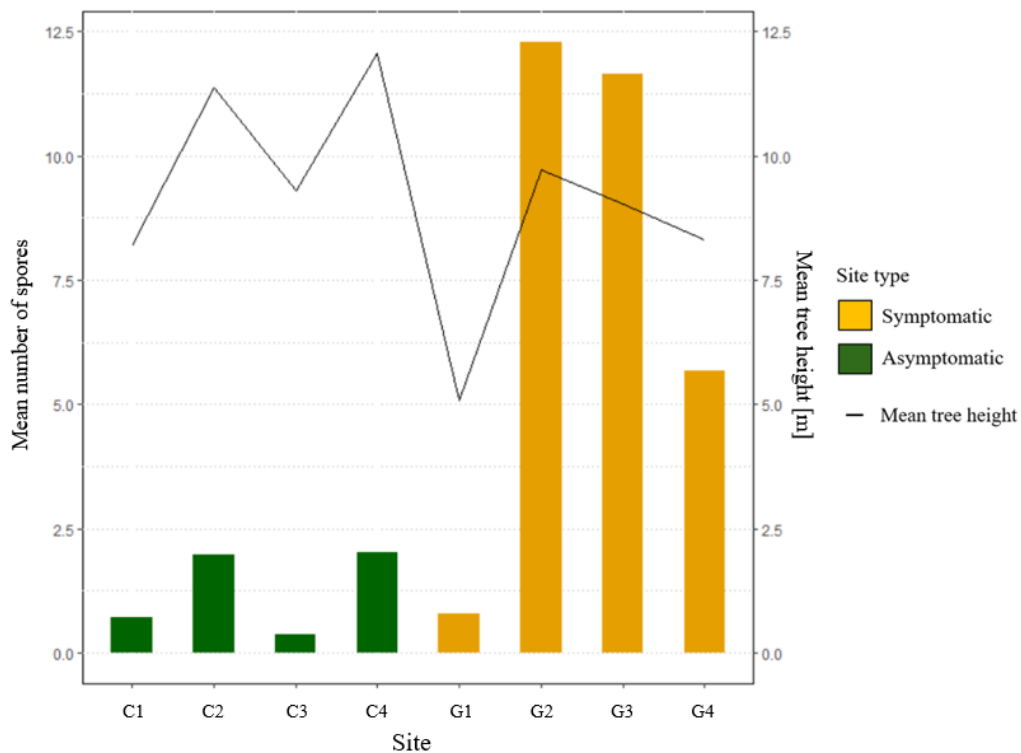


Figure 11. Mean number of spores per site (green bars (C – asymptomatic sites) and yellow bars (G – symptomatic sites)) and mean tree height [m] per site (black line). Variability in spore loads between sites is positively correlated to tree height ($P = 0.020$ *).

3.3. Local climate

Regression parameters for the effect of average daily mean, maximum and minimum relative humidity and temperature during the period December 2018–October 2019 on site condition (symptomatic or asymptomatic) are shown in Table 3. The average daily mean, maximum and minimum relative humidity (RH) during the period was statistically significantly lower at symptomatic sites than at asymptomatic sites. The average daily mean, maximum and minimum temperature during the period did not differ significantly between the site types (see Table 3).

Table 3. Estimated regression parameters for the binomial generalised linear model testing the effect of relative humidity and temperature on site condition (asymptomatic vs symptomatic sites) during the period December 2018-October 2019.

		Estimate (symptomatic sites)	SE	z-value ^a	P-value ^b
RH	Mean	-0.0673	0.0228	-2.956	0.0031 **
	Max	-0.1304	0.0645	-2.021	0.0432 *
	Min	-0.0292	0.0125	-2.327	0.0200 *
Temp	Mean	-0.0104	0.0325	-0.320	0.749
	Max	-0.0011	0.0253	-0.043	0.965
	Min	-0.0398	0.0409	-0.973	0.330

^a Estimate/SE

^b Significant P-values indicated by asterisks (***) < 0.001 < ** < 0.01 < * < 0.05 < . < 0.1)

Results for the linear model testing the correlation between the site condition (symptomatic or asymptomatic) and average daily mean, maximum and minimum relative humidity per month are presented in Table 4. The average daily mean relative humidity was statistically significantly higher at asymptomatic sites than at symptomatic sites in December, September and October (see Fig 12. a-c, Table 4). The average daily maximum relative humidity was statistically significantly higher at asymptomatic sites than at symptomatic sites in December, January and October (see Fig 12. a-c, Table 4), while the average daily minimum relative humidity was statistically significantly higher at asymptomatic sites than at symptomatic sites only in October (Fig. 12. a-c, Table 4).

Table 4. Estimated marginal means on the linear model testing the effect of relative humidity per month on site condition (symptomatic vs asymptomatic sites).

	Month	Estimate (asymptomatic sites)	SE	t-value ^a	P-value ^b	R ^{2c}	Adj. R ^{2d}	df ^e	F ^f	P-value ^g
Mean RH	Dec	9.49	4.34	2.189	0.0323 *	0.7642	0.6843	62	F _(21,62) = 9.567	<0.0001 ***
	Jan	7.04	4.34	1.623	0.1096					
	Feb	4.07	4.34	0.939	0.3512					
	March	2.71	4.34	0.625	0.5342					
	April	3.13	4.34	0.722	0.4728					
	May	3.67	4.34	0.848	0.3999					
	June	4.81	4.34	1.109	0.2719					
	July	8.92	4.68	1.904	0.0616 .					
	Aug	7.58	4.68	1.619	0.1106					
	Sept	9.82	4.68	2.097	0.0401 *					
Oct	23.80	4.68	5.083	<0.0001 ***						
Maximum RH	Dec	8.458	2.68	3.160	0.0024 **	0.5787	0.436	62	F _(21,62) = 4.055	<0.0001 ***
	Jan	6.396	2.68	2.389	0.0199 *					
	Feb	0.778	2.68	0.291	0.7724					
	March	0.326	2.68	0.122	0.9034					
	April	-1.987	2.68	-0.742	0.4607					
	May	-0.797	2.68	-0.298	0.7670					
	June	-0.977	2.68	-0.365	0.7162					
	July	0.655	2.89	0.227	0.8214					
	Aug	0.440	2.89	0.152	0.8795					
	Sept	0.808	2.89	0.279	0.7809					
Oct	13.433	2.89	4.646	<0.0001 ***						
Minimum RH	Dec	9.71	7.91	1.227	0.2244	0.7465	0.6606	62	F _(21,62) = 8.694	<0.0001 ***
	Jan	7.17	7.91	0.906	0.3685					
	Feb	6.97	7.91	0.880	0.3820					
	March	3.78	7.91	0.478	0.6343					
	April	2.69	7.91	0.340	0.7350					
	May	6.62	7.91	0.837	0.4060					
	June	7.53	7.91	0.951	0.3452					
	July	14.31	8.55	1.674	0.0991 .					
	Aug	11.22	8.55	1.313	0.1941					
	Sept	15.25	8.55	1.784	0.0793 .					
Oct	35.88	8.55	4.197	0.0001 ***						

^a Estimate/SE

^b P-value per parameter – significance indicated by asterisks (***) < 0.001 < ** < 0.01 < * < 0.05 < . < 0.1)

^c Variation in x explained by variation in y

^d Adjusted R² – variation in x explained by variation in y – significant variables considered only

^e Degrees of freedom for overall model

^f F-statistic – variation between sample means / variation within the samples (df1, df2)

^g Overall P-value for model – significance indicated by asterisks (***) < 0.001 < ** < 0.01 < * < 0.05 < . < 0.1)

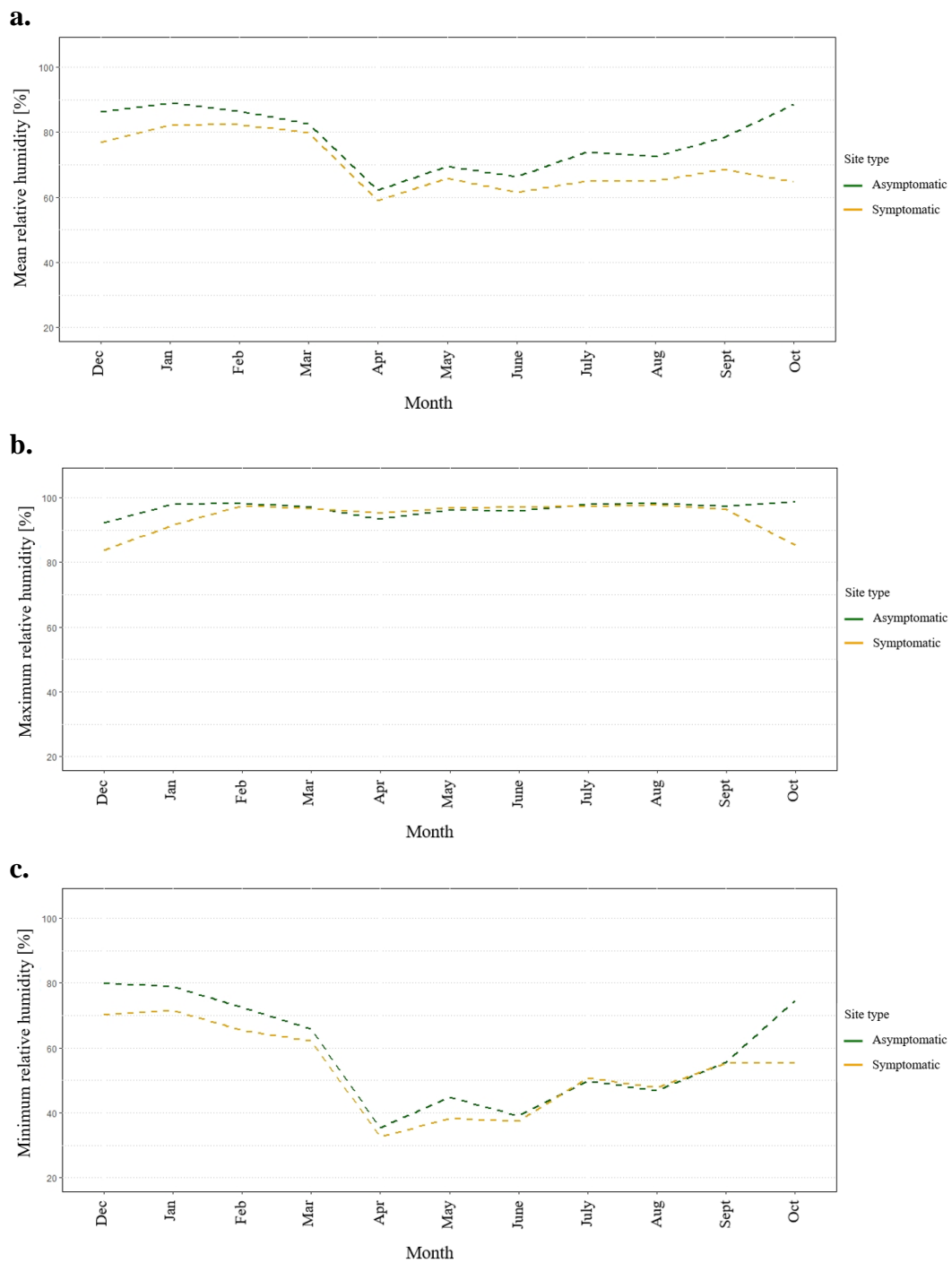


Figure 12. a-c. Average daily mean (a), maximum (b) and minimum (c) relative humidity per month at asymptomatic sites (green dashed lines) and symptomatic sites (yellow dashed lines). Average daily mean relative humidity was higher at asymptomatic sites than at symptomatic sites in December ($P = 0.032$ *), September ($P = 0.040$ *) and October ($P < 0.001$ ***). Average daily maximum relative humidity was higher at asymptomatic sites than at symptomatic sites in December ($P = 0.002$ **), January ($P = 0.020$ *) and October ($P < 0.001$ ***). Average daily minimum relative humidity was higher at asymptomatic sites than at symptomatic sites in October ($P < 0.001$ ***). See also Table 4.

Results for the linear model testing the correlation between the site condition (symptomatic or asymptomatic) and average daily mean, maximum and minimum temperature per month are presented in Table 5.

Table 5. Estimated marginal means on the linear model testing the effect of temperature per month on site condition (symptomatic vs asymptomatic sites).

	Month	Estimate (asymptomatic sites)	SE	t-value ^a	P-value ^b	R ² ^c	Adj. R ² ^d	df ^e	F ^f	P-value ^g
Mean temp	Dec	1.5781	0.219	7.221	<0.0001 ***	0.9984	0.9979	62	F _(21,62) = 1897	<0.0001 ***
	Jan	0.2263	0.219	1.035	0.3045					
	Feb	0.0251	0.219	0.115	0.9089					
	Mar	-0.0599	0.219	-0.274	0.7850					
	Apr	-0.1834	0.219	-0.839	0.4047					
	May	-0.3226	0.219	-1.476	0.1449					
	June	-0.5399	0.219	-2.470	0.0163 *					
	July	-0.5378	0.236	-2.278	0.0262 *					
	Aug	-0.4728	0.236	-2.003	0.0495 *					
	Sept	-0.2262	0.236	-0.958	0.3417					
Oct	-0.0264	0.236	-0.112	0.9112						
Maximum temp	Dec	1.53671	0.885	1.737	0.0874 .	0.9845	0.9792	62	F _(21,62) = 187.4	<0.0001 ***
	Jan	0.00598	0.885	0.007	0.9946					
	Feb	-0.22312	0.885	-0.252	0.8017					
	Mar	-0.43183	0.885	-0.488	0.6272					
	Apr	-0.83759	0.885	-0.947	0.3475					
	May	-0.66300	0.885	-0.749	0.4565					
	June	-0.83946	0.885	-0.949	0.3464					
	July	-0.98481	0.956	-1.030	0.3068					
	Aug	-1.40505	0.956	-1.470	0.1466					
	Sept	-1.07256	0.956	-1.122	0.2661					
Oct	-0.73238	0.956	-0.766	0.4464						
Maximum temp	Dec	1.762	0.385	4.573	<0.0001 ***	0.9925	0.9899	62	F _(21,62) = 390.2	<0.0001 ***
	Jan	0.763	0.385	1.981	0.0521 .					
	Feb	0.338	0.385	0.878	0.3831					
	Mar	0.433	0.385	1.125	0.2651					
	Apr	0.814	0.385	2.112	0.0387 *					
	May	0.512	0.385	1.328	0.1889					
	June	0.459	0.385	1.190	0.2384					
	July	0.572	0.416	1.375	0.1741					
	Aug	0.674	0.416	1.621	0.1101					
	Sept	0.602	0.416	1.447	0.1528					
Oct	0.412	0.416	0.990	0.3261						

^a Estimate/SE

^b P-value per parameter – significance indicated by asterisks (*** < 0.001 < ** < 0.01 < * < 0.05 < . < 0.1)

^c Variation in x explained by variation in y

^d Adjusted R² – variation in x explained by variation in y – significant variables considered only

^e Degrees of freedom for overall model

^f F-statistic – variation between sample means / variation within the samples (df1, df2)

^g Overall P-value for model – significance indicated by asterisks (*** < 0.001 < ** < 0.01 < * < 0.05 < . < 0.1)

The average daily mean temperature was statistically significantly higher at asymptomatic sites than at symptomatic sites in December, and lower at asymptomatic sites than at symptomatic sites in June, July and August (see Fig 13. a-c, Table 5). The average daily maximum temperature did not differ significantly between the site types. The average daily minimum temperature was statistically significantly higher at asymptomatic sites than at symptomatic sites in December and April (Fig. 13. a-c, Table 5).

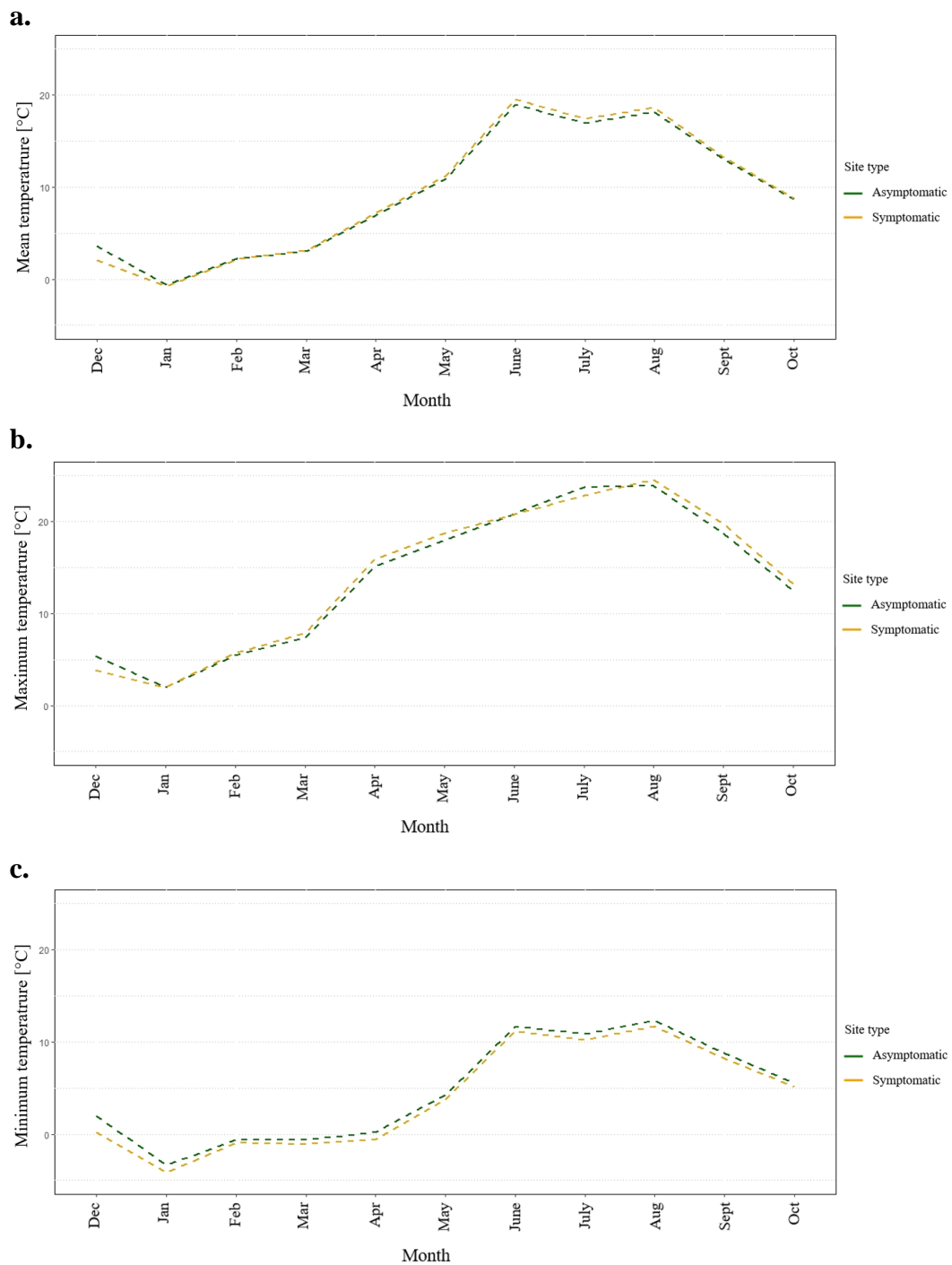


Figure 13. a-c. Average daily mean (a), maximum (b) and minimum (c) temperature per month at asymptomatic sites (green dashed lines), and symptomatic sites (yellow dashed lines). Average daily mean temperature was higher at asymptomatic sites than at symptomatic sites in December ($P < 0.001$ ***), and lower at asymptomatic sites than at symptomatic sites in June ($P = 0.016$ *), July ($P = 0.026$ *) and August ($P = 0.050$ *). Average daily maximum temperature did not differ significantly between the site types. Average daily minimum temperature was higher at asymptomatic sites than at symptomatic sites in December ($P < 0.001$ ***) and April ($P = 0.039$ *). See also Table 5.

3.4. Soil properties

3.4.1. Soil type

The soil type is rock at all four symptomatic sites (G1-G4) and one asymptomatic site (C3). The asymptomatic sites C1 and C4 are located on post-glacial sand/gravel, and C2 is located on clay till (see Fig. 14) (SGU, 2014).

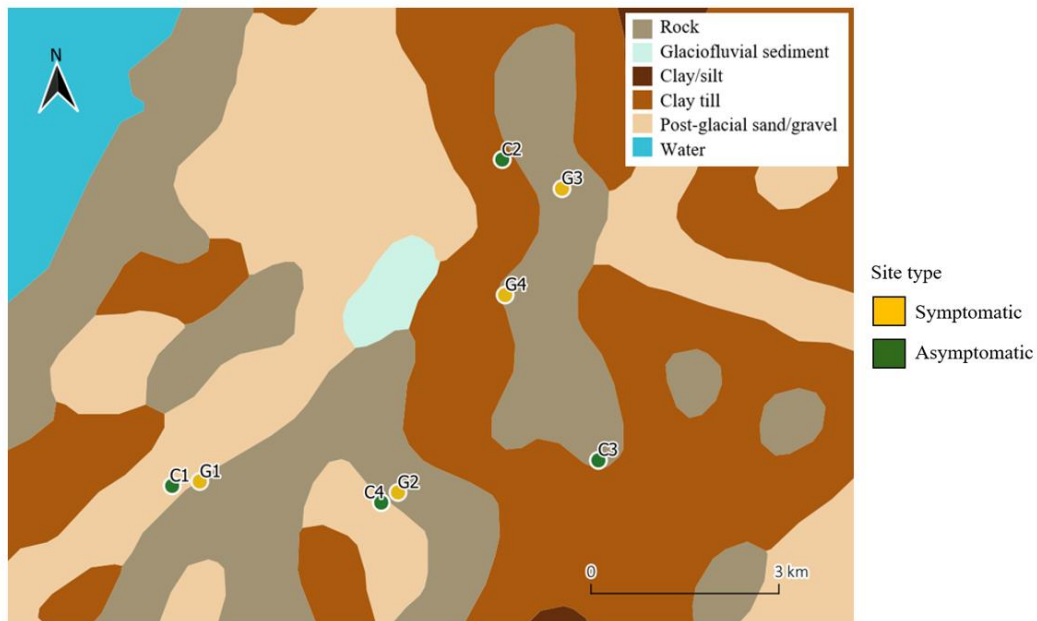


Figure 14. Soil types in the area of the experimental sites (Jordartskartan © SGU). Asymptomatic sites (C1-C4) indicated by green dots and symptomatic sites (G1-G4) indicated by yellow dots. C1 and C4 are located on post-glacial sand/gravel, C2 is located on clay till. All other sites are located on rock.

3.4.2. Soil depth

The average soil depth is 0.0 m at all sites except the asymptomatic site C4, which has an average soil depth of 2.5 m (see Fig. 15) (SGU, 2017).

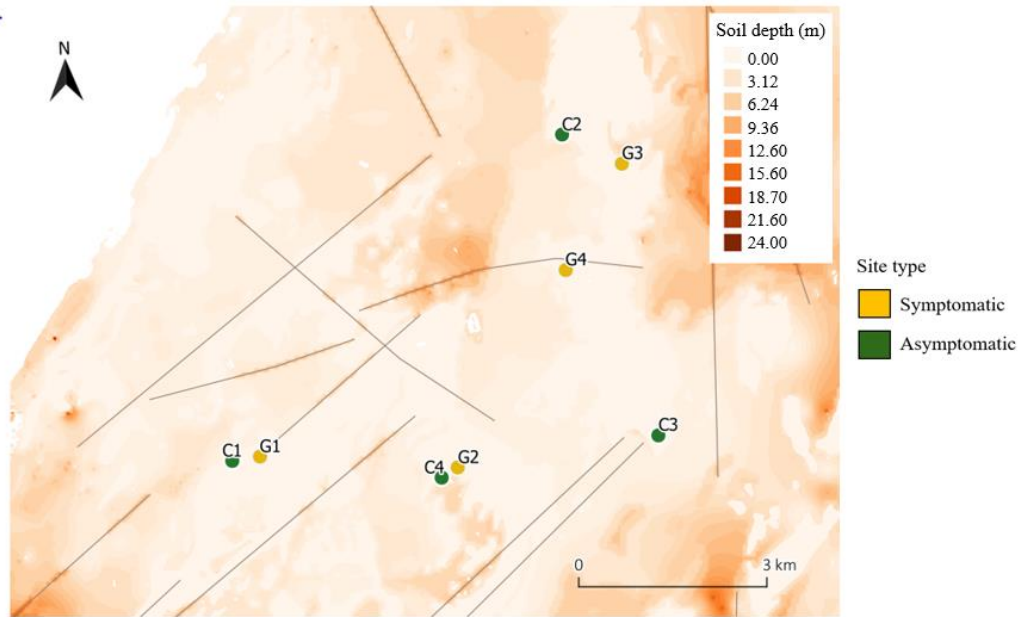


Figure 15. Soil depth and cracks (seen as dark brown lines) in bedrock in the area of the experimental sites (Jorddjupsmodell © SGU). Asymptomatic sites (C1-C4) indicated by green dots and symptomatic sites (G1-G4) indicated by yellow dots. Site C4 has an average soil depth of 2.5 m, and all other sites have an average soil depth of 0.0 m.

3.4.3. Soil nutrients and properties

Results from the laboratory analyses on soil nutrients and properties are presented in Table 6.

Table 6. Laboratory soil analysis results per group. Group definitions: CH – asymptomatic sites, asymptomatic trees; GA – symptomatic sites, symptomatic trees; GH – symptomatic sites, asymptomatic trees.

Site ID	Group ID	pH	NH ₄ (mg/L)	NO ₃ (mg/L)	Inorganic N (mg/L)	P (mg/100g)	K (mg/100g)	Ca (mg/100g)	LoI ^a	WHC ^b
G1	G1H	7.56	4.73	0.09	4.82	0.38	16.00	1953.44	12.67	97.97
G1	G1A	7.49	5.66	0.10	5.76	0.61	39.20	3515.66	17.79	120.72
G2	G2H	5.65	2.47	0.01	2.48	0.76	6.26	114.58	8.02	74.86
G2	G2A	5.91	2.42	0.09	2.51	0.89	9.63	105.38	6.18	64.67
G3	G3H	6.92	10.05	0.24	10.29	1.34	15.05	1582.28	18.40	100.91
G3	G3A	6.78	5.65	0.17	5.82	1.39	13.72	1212.48	15.94	119.01
G4	G4H	6.37	7.38	0.21	7.59	4.03	30.78	1325.02	77.11	294.31
G4	G4A	6.78	10.55	0.73	11.28	1.82	17.57	801.78	23.99	163.04
C1	C1H	6.58	4.19	0.13	4.32	0.59	7.97	280.69	7.96	68.24
C2	C2H	5.54	2.48	0.03	2.51	0.89	10.09	167.22	11.28	87.04
C3	C3H	7.13	9.52	0.27	9.79	1.56	35.58	1648.48	26.77	144.74
C4	C4H	5.92	3.62	0.01	3.63	1.15	8.02	129.27	7.41	73.82

^a Loss on ignition

^b Water-holding capacity (mL H₂O/100 g dry soil)

The soil nutrients and properties showed no significant differences between asymptomatic and symptomatic sites (see Fig. 16), between groups of healthy and affected trees, or between the group types (CH – asymptomatic sites, asymptomatic

trees; GA – symptomatic sites, symptomatic trees; GH – symptomatic sites, asymptomatic trees, see Fig. 17). The variance was lower within the asymptomatic sites than within the symptomatic sites, with the exception of site Control 3 (see Fig. A1+A2 in Appendix 2). Results on statistical analyses for the nutrients and properties of soil are presented in Appendix 2.

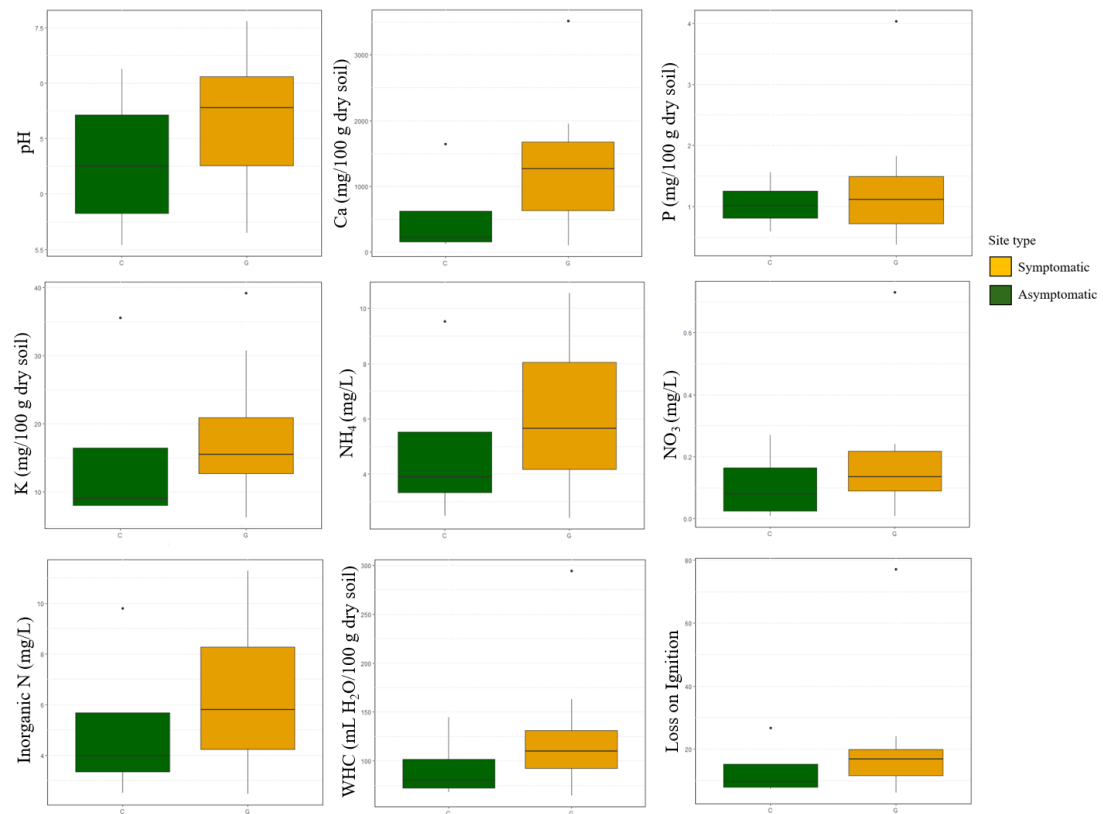


Figure 16. Soil nutrient and property values for asymptomatic sites (green boxes) and symptomatic sites (yellow boxes). From upper left corner: pH, calcium, phosphorus, potassium, ammonium, nitrate, total inorganic nitrogen, water-holding capacity and loss on ignition. All values are higher at symptomatic sites than at asymptomatic sites, although no differences are statistically significant.

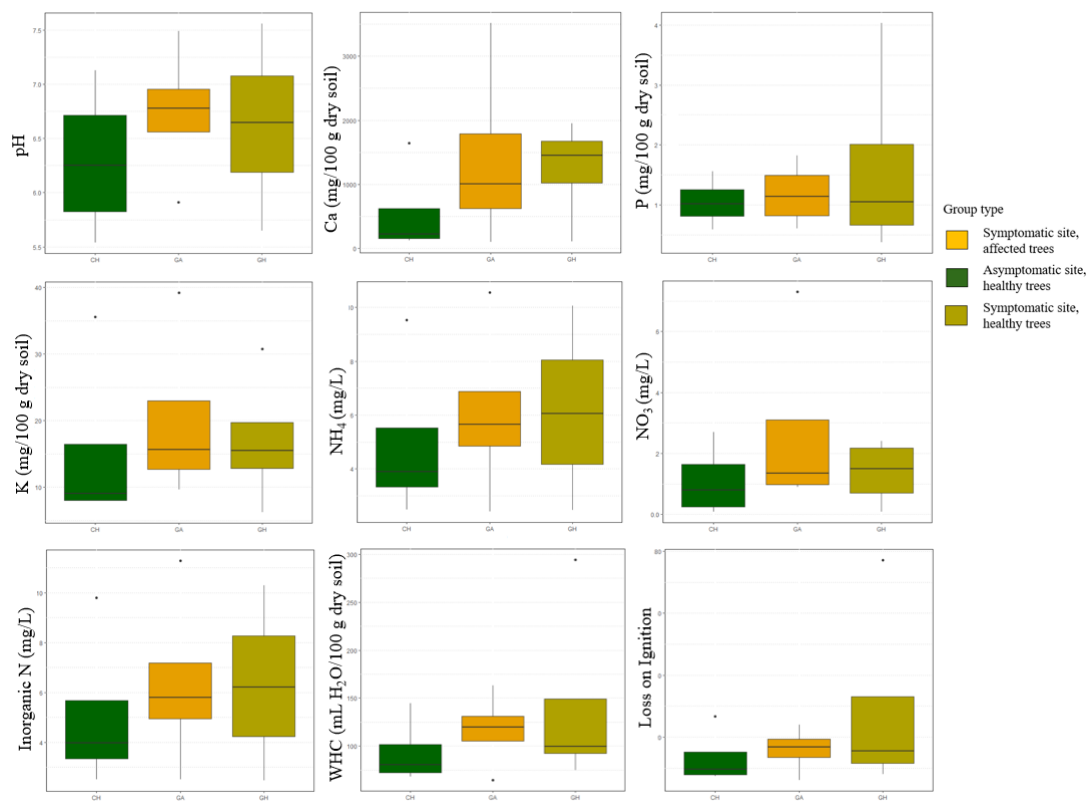


Figure 17. Soil nutrient and property values for healthy trees at asymptomatic sites (group CH, green boxes), affected trees at symptomatic sites (group GA, yellow boxes) and for healthy trees at symptomatic sites (group GH, light green boxes). From upper left corner: pH, calcium, phosphorus, potassium, ammonium, nitrate, total inorganic nitrogen, water-holding capacity and loss on ignition. None of the soil nutrients and properties are statistically significantly different between the group types.

4. Discussion

4.1. The analyses

4.1.1. Studied trees: Tree damage

The hypothesis that trees with a lower level of defoliation have a higher chance of recovering after a rapid decline and vice versa was rejected. In general, trees did not recover the year after the drought, and trees at symptomatic sites with low levels of damage shortly after the decline was discovered rarely kept those low levels the following year. The increase in defoliation during 2019 was slightly larger in trees that had a high level of defoliation directly after the drought in 2018. It is possible that the trees would have had the power to recover if the pathogen pressure was lower or the drought less severe, but together, the stressors appear too much for some of the trees.

None of the trees at the asymptomatic sites showed any defoliation during the first damage estimation in 2018, but individual trees at all four sites displayed low levels of defoliation when damage estimation was performed the second year. Control 3 was the asymptomatic site with the highest level of defoliation in 2019.

The results may be affected by the difficulty distinguishing different high levels of defoliation, while differences between healthy and slightly defoliated trees are easier to see by eye. The results do not prove that trees that look healthy after an outbreak should always be expected to get severely damaged, but in this case, the symptoms might have been delayed and not visible until later. Another aspect is that the comparison is difficult to make because already dead needles might fall off before the next year's damage estimation and the remaining crown looks green although it did not recover. Also, blight is difficult to see in direct sunlight and when the sky is cloudy but bright. Depending on where the sun is, one may see defoliation well on one side of the crown but miss it on the other side. It is easier to visually detect defoliation from a distance compared to in an angle from below. However, in stands with high densities, some trees must be examined from close by.

Damage estimations using drones would be a good alternative to estimation by eye from the ground. Images would make it easier to compare different sites, and they could be analysed by several people or by a computer.

4.1.2. Spore loads

As hypothesised, symptomatic sites showed higher spore loads than asymptomatic sites overall, but the hypothesis had to be rejected for some seasons. Considering the correlation between precipitation and number of spores (Fig. 10 in the Results section), it is likely that the lack of precipitation explains the low spore load at all sites in April. During the first spore trap week in autumn, most of the precipitation came on the last day, potentially explaining the lower correlation between spore load and precipitation during that period. Also, since *D. sapinea* infects young tissue, the fungi should be more active after flushing (occurring in late spring for *P. sylvestris*), which may contribute to the significantly higher spore loads in summer compared to the other seasons.

The fact that spores were found at all asymptomatic sites strengthen the idea of *D. sapinea* existing as a latent pathogen or an endophyte. Studies have shown that approximately 2/3 of the spores are lost when using the method of isolating DNA from filter papers described in this thesis (Dr. Ke Zhang, personal communication (unpublished data)), so the low number of spores detected in some of the traps are not negligible. The same study showed that the number of spores on filter paper is positively correlated to qPCR quantification of spores ($R^2 = 0.9844$), confirming the reliability in the method of determining the abundance of spores in filter paper spore traps (Dr. Ke Zhang, personal communication (unpublished data)).

Although symptomatic sites had higher spore loads than asymptomatic sites overall, there were exceptions. The trees at site Gotland 1 generally had a high level of defoliation, but the spore traps showed a continuously low spore load, in the same range as site Control 1. Control 2 and Control 4 were almost free from defoliation also in the second damage estimation but had higher spore loads than Gotland 1. Why the difference between symptomatic and asymptomatic sites was not more apparent can be partly explained by the affect tree height seem to have on the efficiency of the spore trapping (see Fig. 11 in the Results section). Due to the large size of the *D. sapinea* spores, which reduces their capacity to spread long distances (Norros *et al.*, 2014), the spores from lower trees may simply not reach the traps. It could also mean that heavy spore load of *D. sapinea* in some locations is not as worrisome as it seems for the forests on Gotland where trees are not so tall, since the spores spread relatively short distances.

In order to appropriately account for the effect of tree height on trapped spores in future studies, it would be recommended to calculate an index comprising height and distance measurements regarding tree and trap positioning.

4.1.3. Local climate

A priori, it was hypothesised that relative humidity is higher at asymptomatic sites than at symptomatic sites. *A posteriori*, this is the impression one gets from visiting the sites – the amount and type of ground vegetation differ, not surprisingly, and the asymptomatic sites are moister – and it is also what the results show. Although *D. sapinea* require high humidity to infect tissue, the long-term average humidity seems to benefit the pines more.

The mean temperature was higher at asymptomatic sites than at symptomatic sites in December, and lower at asymptomatic sites than at symptomatic sites in June, July and August. A difference in temperature between the sites was not expected since they are located in such proximity, but this shows that trees at asymptomatic sites were exposed to less extremes in temperature, presumably beneficial for the trees.

Data has been processed according to the Tinytag logger manufacturer, by deleting abnormal peaks and drops in relative humidity (>100% and <0%). Consequently, a large number of measurements had to be erased. To exclude potential bias, it should be further investigated why those abnormalities occurred and if they did so more often in a certain type of site.

4.1.4. Soil properties

Soil sampling for forestry has some limits in its use. Trees integrate nutrient availability throughout the soil profile thanks to their extensive, perennial root systems, and it is difficult to obtain a representative sample due to the complex nutrient stratification in forest soils. Further, it is complicated to correlate soil test levels with timber yields due to the long time frame (Brady and Weil, 2008). Therefore, foliar analysis is more useful in forestry, while soil testing is more reliable for agricultural systems. However, soil tests can still be suitable for identifying soils with or without adequate ability to supply nutrients, especially P and K (Brady and Weil, 2008). In this study, soil analysis was used as the interest was in the soil properties and how they affect the health of the trees. The nutrient content of the leaves is altered post infection and drought, and foliar analysis would thereby not give much information about why the trees at some sites are affected. The small size of the experimental sites also gave a better opportunity to sample representative soil than what would be the case in large forest areas.

Although the results from the soil analyses did not show any significant differences between healthy and affected trees, it cannot be ruled out that the nutrients and properties play a major role in the health of those pines. It was unfortunate that the soil samples had to be pooled, and that so few datapoints were achieved. In hindsight, it would have been a good idea to analyse the soil depth data before performing soil sampling in the field. Although the data did not give information about the exact soil depth available for each individual tree, it did give a good indication of the difficulties we were to expect when sampling.

Considering the soil type and soil depth data (see Fig. 14 and Fig. 15 in the Results section), it is clear that some soil is better for the trees than no soil. Control 3 is the only asymptomatic site located on the soil type rock and, as mentioned before, it was the asymptomatic site with the highest level of defoliation in 2019.

4.1.5. Conclusion results

The results show that the site at which a tree is located profoundly affects its tolerance to biotic stressors. The sites in this study are all located within an equilateral 8-kilometre triangulated area (see Fig. 4 in the Materials and Methods section), with similar climate. The most prominent difference between symptomatic sites and asymptomatic sites is the soil type, specifically the lack of soil (exposed bedrock). Although relatively detailed data on soil depth was employed, it showed that the soil in the area is very thin (0.0 m on average at all sites except site C4, see Fig. 15 in the Results section) but did not enable analyses of the conditions for the individual trees. With minimal soil supplied, the trees must rely on high enough nutrient and water content in the soil that accumulates in cracks in the bedrock. Maybe that explains why the symptomatic sites, as oppose to the hypothesis, showed higher values of all analysed nutrients as well as organic matter and water-holding capacity – without the relatively “good” properties of that soil, the trees would not be able to grow at all. The soil also explains the differences in local relative humidity, since scarce ground vegetation and exposed bedrock increases the speed of the ground drying up.

It will be interesting to follow the development in site Control 3, as the site shares many characteristics with the symptomatic sites; soil type, soil properties (see Fig. A1+A2 in Appendix 2), and increased defoliation the year after the *D. sapinea* outbreak). It could provide interesting individuals for further studies since the trees are relatively healthy, although the factors mentioned above speak against it.

4.2. The outbreak of *D. sapinea* on Gotland

Drought is frequent on Gotland, and the low ground-water levels require the population on parts of the island to restrict their water use almost every summer. The trees are exposed to dry periods as often and are presumably adapted to those periods. However, the summer of 2018 was extreme, and Gotland did not receive any precipitation for several months (Swedish Meteorological and Hydrological Institute, 2020). In autumn 2018, the ground-water level was lower than in over 30 years (see Fig. 18) and stayed at maximum low for longer than usual (see Fig. 19) (SGU, 2020). Considering the stress that the extensive drought put on trees in the most affected locations on the island, it is not surprising that *D. sapinea* strived during 2018. The ground-water level measured in autumn 2019 reached even lower levels (see Fig. 18) (SGU, 2020), thus potentially hindering the recovery of the stressed pines.

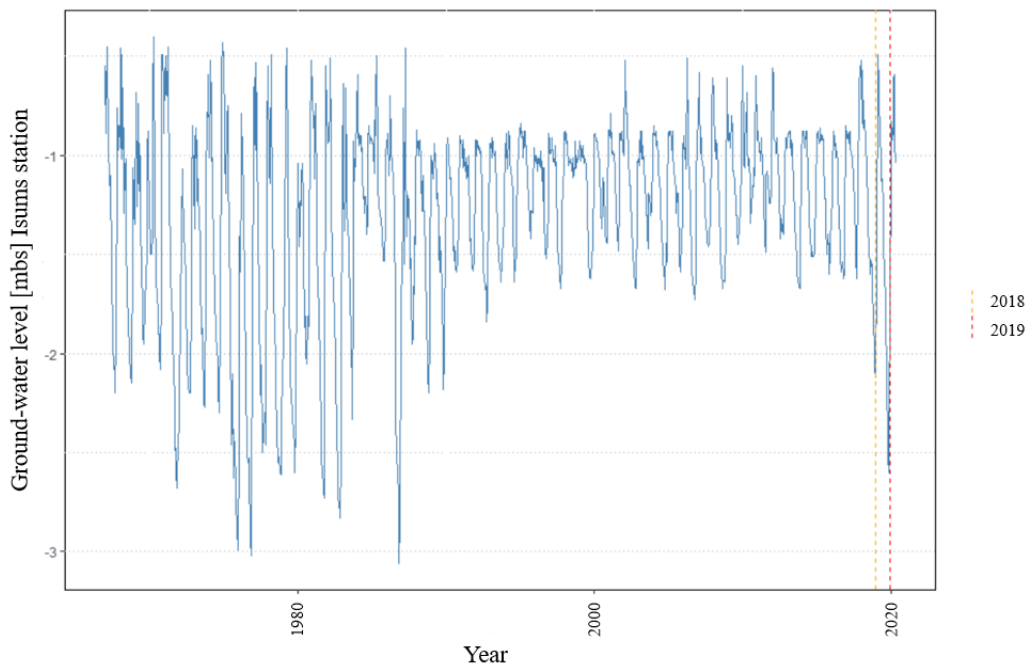


Figure 18. Ground-water levels (meters below surface) at Isums station recorded from 1967 to 2020. The ground-water level in autumn 2018 (indicated by yellow dashed line) was lower than in over 30 years and reached even lower levels in autumn 2019 (indicated by red dashed line) (SGU, 2020).

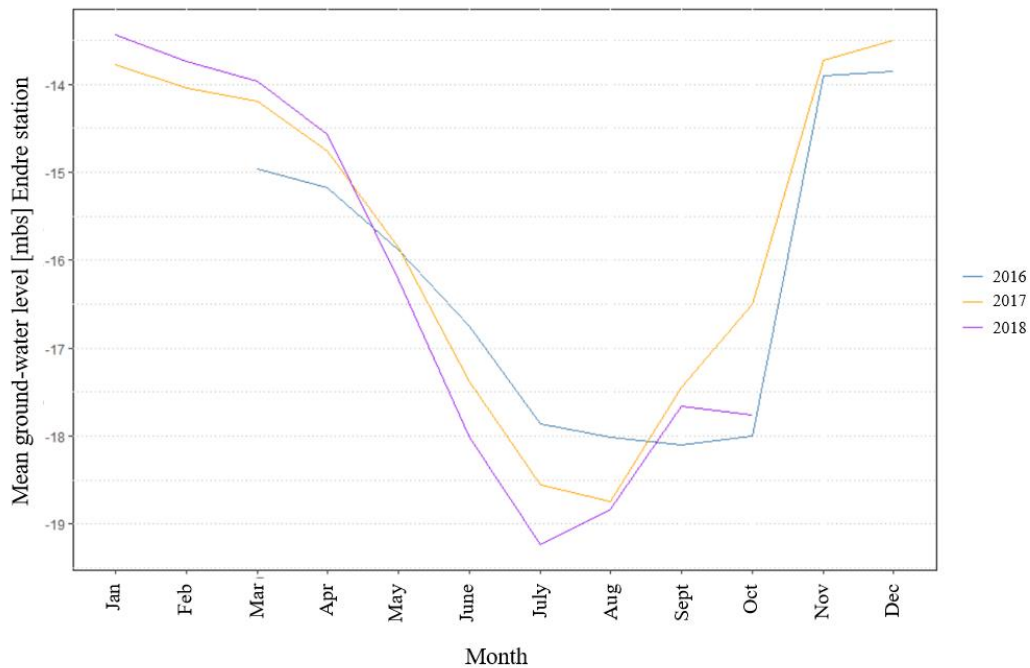


Figure 19. Ground-water levels (meters below surface) at Endre station recorded from March 2016 to October 2018, showing that the levels in 2018 (purple line) were lower than the prior years (SGU, 2020).

4.3. Future

According to Persson *et al.* (2015), the future climate on Gotland will be warmer, with an annual average temperature increasing from today's 7.5-8.0°C to 9.5-10.0°C in the year 2098 if emissions decrease, and to above 11°C if emissions continue to increase. The average annual precipitation was 634 mm between 1961 and 1990, which is predicted to increase to 760 mm 2069-2098 if emissions are decreased, and to 825 mm if emissions remain to increase. The growing period occurred between mid-April and mid-November 1961-1990, but is expected to last from the beginning of March to mid-December the year 2069-2098 with lowered emissions and from the beginning of February to the end of December 2069-2098 if emissions to the atmosphere are not slowed down (Persson *et al.*, 2015).

A warmer and wetter climate is, as mentioned in the introduction, not expected to change the impact by *D. sapinea* (Sturrock *et al.*, 2011). With a considerably longer growing period in the future, the impact of *D. sapinea* may still increase since fungal pathogens have a higher ability to adapt to new environmental conditions than their host trees, as stated by Sturrock *et al.* (2011). The change in temperature and precipitation will presumably also lead to more extreme weather, including drought periods (Persson *et al.*, 2015), favouring pathogens like *D. sapinea*.

Diplodia sapinea is not the only threat to the Scots pines on Gotland. The fungus *Heterobasidion annosum* have recently been identified as the causal agent to damages in many pine stands on the island (SVT Nyheter, 2020). Drought also promotes large-scale tree mortality induced by insects (Huang *et al.*, 2020), which the island already seem to experience; during 2019, we found traces of bark beetle attacks at the symptomatic sites. It is unclear if those insects were secondary to the fungus or not, but regardless, they constitute yet another layer of stress to the trees.

Gonthier (2013) suspects that the role of forest diseases in forest decline may be underestimated due to our incapacity to see the agents that cause diseases, as opposed to our ability to visually recognise and detect events such as forest fires or storms. If that is the case, more knowledge is needed for forest owners and stakeholders.

We need to further characterise the stress responses in pines, both molecular and physiological, to be able to predict how climate change will affect forest health in the future. This is especially important since traits selected for drought tolerance may compromise defences against biotic stressors such as pathogens (Sherwood *et al.*, 2015).

Already 30 years ago, Nicholls and Ostry (1990) stated that the most important measure to control *D. sapinea* is to consider the risk of planting pines on poor sites since it can expose the trees to stresses that predispose infection by the fungus. According to Capretti *et al.* (2013), *D. sapinea* can be controlled by avoiding stagnant water, removing sources of inoculum (such as infected cones and twigs in the trees or on the ground), and maintaining tree health. Even though Scots pine is a very tolerant tree and traditionally has been seen as the best choice of tree species financially when the site is dry and low in nutrient supply (Albrektsson *et al.*, 2012; Heurgren Film, 2019), I think the predicted environmental change will lead to this view becoming highly counterproductive for Swedish forests.

4.4. Conclusion

Replacing Scots pine in plantations with another tree species may be a long-term option to make up for its economic value for forestry, but its ecological value is irreplaceable. With a changing climate, changed distributions of pests and pathogens, and a potentially increased impact of diseases such as *Diplodia* shoot blight, it may be time to stop viewing Scots pine as a tree one can plant at poor sites. We should instead strive to plant the tree where it has soil properties, nutrition and water supply that match its needs. Selecting suitable sites will give healthy trees

that are able to withstand periods of stress and threats, like the one on Gotland, which are inevitable in the future.

The relationship between the abiotic drought stress and the biotic *D. sapinea* outbreak appears to be causal rather than correlating, with drought being a strong driver of the degree of infection and site properties clearly affecting the extent of the impact of the drought on the trees. Conclusively, the interactions between nutrient-limited pine trees, drought, and the pathogen constitute a complete disease triangle.

References

- Agrios, G. N. (2005) *Plant Pathology*. 5th edn. London: Academic Press.
- Albrektsson, A. *et al.* (2012) *Skogsskötselns grunder och samband*.
- Bachi, P. R. and Peterson, J. L. (1985) 'Enhancement of *Sphaeropsis sapinea* Stem Invasion of Pines by Water Deficits', *Plant Disease*, 69(9), pp. 798–799.
- Blodgett, J. T., Herms, D. A. and Bonello, P. (2005) 'Effects of fertilization on red pine defense chemistry and resistance to *Sphaeropsis sapinea*', *Forest Ecology and Management*, 208(1–3), pp. 373–382. doi: 10.1016/j.foreco.2005.01.014.
- Blodgett, J. T., Kruger, E. L. and Stanosz, G. R. (1997a) 'Effects of moderate water stress on disease development by *Sphaeropsis sapinea* on red pine', *Phytopathology*, 87(4), pp. 422–428. doi: 10.1094/PHYTO.1997.87.4.422.
- Blodgett, J. T., Kruger, E. L. and Stanosz, G. R. (1997b) '*Sphaeropsis sapinea* and water stress in a red pine plantation in Central Wisconsin', *Phytopathology*, 87(4), pp. 429–434. doi: 10.1094/PHYTO.1997.87.4.429.
- Blodgett, J. T. and Stanosz, G. R. (1999) 'Differences in Aggressiveness of *Sphaeropsis sapinea* RAPD Marker Group Isolates on Several Conifers', *Plant Disease*, (September 1999). doi: 10.1094/PDIS.1999.83.9.853.
- Bosso, L. *et al.* (2017) 'Predicting current and future disease outbreaks of *Diplodia sapinea* shoot blight in Italy: species distribution models as a tool for forest management planning', *Forest Ecology and Management*. Elsevier B.V., 400, pp. 655–664. doi: 10.1016/j.foreco.2017.06.044.
- Brady, N. C. and Weil, R. R. (2008) *The Nature and Properties of Soil*. 14th edn. Pearson Education Ltd.
- Brodde, L. *et al.* (2019) 'Diplodia Tip Blight on Its Way to the North : Drivers of Disease Emergence in Northern Europe', 9(January). doi: 10.3389/fpls.2018.01818.
- Brookhouser, L. W. and Peterson, G. W. (1971) 'Infection of Austrian, Scots and Ponderosa pines by *Diplodia pinea*', *Phytopathology*, 61.
- Butin, H. (1989) *Krankheiten der Wald- und Parkbäume. Diagnose-Biologie-Bekämpfung*. 2nd edn. Stuttgart: Georg Thieme Verlag.
- CABI (2019) *Sphaeropsis sapinea (Sphaeropsis blight)*, *Invasive Species Compendium*. Available at: <https://www.cabi.org/isc/datasheet/19160>.
- CABI (2020) *Sphaeropsis sapinea (Sphaeropsis blight) - distribution map*, *Invasive Species Compendium*. Available at:

- <https://www.cabi.org/isc/datasheet/19160#toDistributionMaps> (Accessed: 2 August 2020).
- Capretti, P. *et al.* (2013) 'Branch and tip blights', in Gonthier, P. and Nicolotti, G. (eds) *Infectious Forest Diseases*. CABI Publishing, pp. 420–435. doi: 10.1079/9781780640402.0420.
- Chou, C. K. S. (1976) 'A shoot dieback in *Pinus radiata* caused by *Diplodia pinea* II: Inoculation studies', *New Zealand Journal of Forestry Science*, 6(3), pp. 409–420.
- Dietze, M. C. *et al.* (2014) 'Nonstructural carbon in woody plants', *Annual Review of Plant Biology*, 65, pp. 667–687. doi: 10.1146/annurev-arplant-050213-040054.
- van Dijk, H. F. G. *et al.* (1990) 'Impact of artificial, ammonium-enriched rainwater on soils and young coniferous trees in a greenhouse. Part II- Effects on the trees', *Environmental Pollution*, 63(1), pp. 41–59. doi: 10.1016/0269-7491(90)90102-I.
- Edmonds, R. L. (2013) 'General Strategies of Forest Disease Management', in *Infectious Forest Diseases*. CABI Publishing, pp. 29–49.
- Evert, R. F., Eichhorn, S. E. and Raven, P. H. (2004) *Biology of Plants*. 7th edn. W. H. Freeman.
- Fabre, B. *et al.* (2011) 'Can the emergence of pine *Diplodia* shoot blight in France be explained by changes in pathogen pressure linked to climate change?', *Global Change Biology*, 17(10), pp. 3218–3227. doi: 10.1111/j.1365-2486.2011.02428.x.
- Fridman, J. (2005) 'Broadleaved tree species in conifer-dominated forestry : Regeneration and limitation of saplings in southern Sweden', 214, pp. 142–157. doi: 10.1016/j.foreco.2005.04.001.
- Gonthier, P. (2013) 'Introduction to Infectious Forest Diseases', in Gonthier, P. and Nicolotti, G. (eds) *Infectious Forest Diseases*. CABI Publishing, pp. xxi–xxiii.
- Govrin, E. M. and Levine, A. (2000) 'The hypersensitive response facilitates plant infection by the necrotrophic pathogen *Botrytis cinerea*', *Current Biology*, 10(13), pp. 751–757. doi: 10.1016/S0960-9822(00)00560-1.
- Hamilton, J. G., Arthur, R. and Delucia, E. H. (2001) 'The carbon \pm nutrient balance hypothesis : its rise and fall', *Ecology Letters*, (4), pp. 86–95.
- Hammond-Kosack, K. E. and Rudd, J. J. (2008) 'Plant resistance signalling hijacked by a necrotrophic fungal pathogen', *Plant Signaling and Behavior*, 3(11), pp. 993–995. doi: 10.4161/psb.6292.
- Harding, D. E. and Ross, D. J. (1964) 'Some factors in low-temperature storage influencing the mineralisable-nitrogen of soils', *Journal of the Science of Food and Agriculture*, 15(12), pp. 829–834. doi: 10.1002/jsfa.2740151203.
- Heurgren Film (2019) *Tall, gran eller både och?* Sweden: Skogforsk. Available at: skogforsk.se/kunskap/kunskapsbanken/2019/tall-gran-eller-bade-och/.

- Huang, J. *et al.* (2020) 'Viewpoints Tree defence and bark beetles in a drying world : carbon partitioning , functioning and modelling', *New Phytologist*, (225), pp. 26–36. doi: 10.1111/nph.16173.
- Ingestad, T. (1978) 'silvestris and Picea abies Seedlings', (9), pp. 373–380.
- de Kam, M. *et al.* (1991) 'Effects of fertilization with ammonium sulphate and potassium sulphate on the development of Sphaeropsis sapinea in Corsican pine', *Netherlands Journal of Plant Pathology*, 97(5), pp. 265–274. doi: 10.1007/BF01974222.
- Lantmäteriet (2016) 'GSD-Terrängkartan'.
- Lindén, B. (1981) *Rapport 137: Ammonium- och nitratkvävet rörelser och fördelning i marken. II. Metoder för mineralkväveprovtagning och – analys.*
- Lindén, B. (2013) *Rapport 11: Metoder för förvaring och homogenisering av jordprover vid bestämning av mineralkväve.*
- Lindner, R. C. and Harley, C. P. (1944) 'Nutrient Interrelations in Lime-Induced Chlorosis', *Plant Physiology*, 19(3), pp. 420–439.
- Lindroos, O. (2001) *Underlag för skogligt länsprogram Gotland.* Umeå.
- Luchi, N. *et al.* (2005) 'A Real-Time Quantitative PCR Assay for the Detection of Sphaeropsis sapinea from Inoculated Pinus nigra Shoots', 42, pp. 37–42.
- Molin, N., Persson, M. and Persson, S. (1961) *Root Parasites on Forest Tree Seedlings - Some exploratory tests of the resistance of germinant seedlings and the virulence of some potential parasites, Meddelande från Statens Skogsforskningsinstitut.*
- Nicholls, T. H. and Ostry, M. E. (1990) 'Sphaeropsis sapinea Cankers on Stressed Red and Jack Pines in Minnesota and Wisconsin', *Plant Disease*, 74(1), pp. 54–56. doi: 10.1094/PD-74-0054.
- Norros, V. *et al.* (2014) 'Do small spores disperse further than large spores?', *Ecology*, 95(6), pp. 1612–1621. doi: 10.1890/13-0877.1.
- Oliva, J. *et al.* (2013) 'Concepts of Epidemiology of Forest Diseases', in Gonthier, P. and Nicolotti, G. (eds) *Infectious Forest Diseases.* CABI Publishing, pp. 1–28.
- Oliva, J., Boberg, J. and Stenlid, J. (2013) 'First report of Sphaeropsis sapinea on Scots pine (Pinus sylvestris) and Austrian pine (P. nigra) in Sweden', (August). doi: 10.5197/j.2044-0588.2013.027.023.
- Palmer, M. A. (1987) 'Variation Among Isolates of Sphaeropsis sapinea in the North Central United States ', *Phytopathology*, 77(6), p. 944. doi: 10.1094/phyto-77-944.
- Paoletti, E., Danti, R. and Strati, S. (2001) 'Pre- and post-inoculation water stress affects Sphaeropsis sapinea canker length in Pinus halepensis seedlings', *Forest Pathology*, 31(4), pp. 209–218. doi: 10.1046/j.1439-0329.2001.00237.x.
- Pavloušek, P. (2010) 'Lime-induced chlorosis and drought tolerance of grapevine rootstocks', LVIII(5), pp. 431–440.
- Persson, G. *et al.* (2015) *Framtidsklimat i Gotlands län.*

- Phillips, A. J. L. *et al.* (2013) ‘The Botryosphaeriaceae: Genera and species known from culture’, *Studies in Mycology*. CBS-KNAW Fungal Biodiversity Centre, 76, pp. 51–167. doi: 10.3114/sim0021.
- Pyhäjärvi, T. and Kujala, S. T. (2020) ‘275 years of forestry meets genomics in *Pinus sylvestris*’, (November 2018), pp. 11–30. doi: 10.1111/eva.12809.
- QGIS Development Team (2019) ‘QGIS Geographic Information System’. Available at: <http://qgis.osgeo.org>.
- R Core Team (2018) ‘R Studio’. Vienna: R Foundation for Statistical Computing. Available at: <https://www.r-project.org/>.
- Sancho-Knapik, D. *et al.* (2017) ‘Changes of secondary metabolites in *Pinus sylvestris* L. needles under increasing soil water deficit’. *Annals of Forest Science*. doi: 10.1007/s13595-017-0620-7.
- SGU (2014) ‘Jordarter 1:1 miljon’. Geological Survey of Sweden.
- SGU (2017) ‘Jorddjupsmodell’. Geological Survey of Sweden.
- SGU (2020) *Grundvattennivåer, tidsserier, Geological Survey of Sweden*. Available at: <https://apps.sgu.se/kartvisare/kartvisare-grundvattenniva.html> (Accessed: 2 August 2020).
- Shao, H. *et al.* (2008) ‘Water-deficit stress-induced anatomical changes in higher plants ☆’, 331, pp. 215–225. doi: 10.1016/j.crv.2008.01.002.
- Sherwood, P. *et al.* (2015) ‘Mechanisms of induced susceptibility to *Diplodia* tip blight in drought-stressed Austrian pine’, pp. 549–562. doi: 10.1093/treephys/tpv026.
- Sinclair, W. A. and Hudler, G. W. (1988) ‘Tree declines: four concepts of causality’, *Journal of Arboriculture*, (14), pp. 29–35.
- Skilling, D. D. (1990) *Scotch pine, Silvics of North America: Volume 1. Conifers*. Available at: https://www.srs.fs.usda.gov/pubs/misc/ag_654/volume_1/pinus/sylvestris.htm (Accessed: 2 June 2020).
- Stanosz, B. G. R. *et al.* (2004) ‘Sphaeropsis shoot blight and altered nutrition in red pine plantations treated with paper mill waste sludge’, 34, pp. 245–253.
- Stanosz, G. R. *et al.* (2001) ‘Water stress and *Sphaeropsis sapinea* as a latent pathogen of red pine seedlings’, pp. 531–538.
- Sturrock, R. N. *et al.* (2011) ‘Climate change and forest diseases’, (October 2018). doi: 10.1111/j.1365-3059.2010.02406.x.
- SVT Nyheter (2020) ‘Larmrapport om talldöd på Gotland’, *SVT Nyheter*, 23 March. Available at: <https://www.svt.se/nyheter/lokalt/ost/aggressiv-rotticka-tros-doda-tallar-pa-gotland>.
- Swedish Forest Agency (2020) *Statistikdatabas*. Available at: http://pxweb.skogsstyrelsen.se/pxweb/sv/Skogsstyrelsens_statistikdatabas/Skogsstyrelsens_statistikdatabas__Skogsplantor/?rxid=03eb67a3-87d7-486d-acce-92fc8082735d (Accessed: 4 June 2020).

- Swedish Meteorological and Hydrological Institute (2020) *Väderdata och statistik*. Available at: <https://www.smhi.se/professionella-tjanster/professionella-tjanster/statistik-och-data/vaderdata-och-statistik-1.34242>.
- Swedish National Forest Inventory (2019) *Riksskogstaxeringen*. Available at: skogsstatistik.slu.se/pxweb/sv/ (Accessed: 4 June 2020).
- Swedish University of Agricultural Sciences (2020a) *Markfysiklab*. Available at: slu.se/institutioner/mark-miljo/laboratorier/markfysiklab/ (Accessed: 2 August 2020).
- Swedish University of Agricultural Sciences (2020b) *Markkemi - pH, Markinfo*. Available at: <https://www.slu.se/miljoanalys/statistik-och-miljodata/miljodata/webbtjanster-miljoanalys/markinfo/markinfo/markkemi/ph/> (Accessed: 2 August 2020).
- Zwolinski, J. B., Swart, W. J. and Wingfield, M. J. (1990) 'Economic impact of a post-hail outbreak of dieback induced by *Sphaeropsis sapinea*', *European Journal of Forest Pathology*, 20(6–7), pp. 405–411. doi: 10.1111/j.1439-0329.1990.tb01155.x.

Acknowledgements

I would like to thank my supervisors Laura Brodde, Jan Stenlid and Malin Elfstrand for their inexhaustible support during this project. Further, I am also grateful to Karin Wågström and the Swedish Forest Agency on Gotland for making this project possible, Cecilia Bandh and Elin Ljunggren for helping out with soil analyses, and Mireia Gomez-Gallego for many hours of online-based lectures in statistics and R. I thank Eddy, Katta, Rena and the other Mykopats for being excellent colleagues and mentors. I also want to thank Michelle and Sebastian for friendly and scientific advice, Mum and Ulf for providing us with a private B&B/research station on Gotland, and Irma for always looking out for me.

Appendix

Appendix 1.

Studied trees

Table A1. Table showing diameter breast height [cm], height [m]), defoliation in 2018 and 2019, and the presence of bifurcation for each tree included in the study.

Tree ID	Site type	Site	Diameter breast height [cm]	Height [m]	% defoliation 2018	% defoliation 2019	% defoliation residual crown	Bifurcation (1/0)
1	G	G1	8.5	5.2	0.05	0	-0.05	0
2	G	G1	10.5	4.5	0.3	0.4	0.14	1
3	G	G1	8.5	4.5	0.05	0	-0.05	0
4	G	G1	7.5	3	1	1	0.0	1
5	G	G1	15	6.5	0.05	0.05	0.0	0
6	G	G1	7	4.5	0.3	0.8	0.71	0
7	G	G1	8.5	6	0.05	0.05	0.0	0
8	G	G1	15	4	0.8	1	1.0	1
9	G	G1	10.5	4.5	0.05	0.2	0.16	0
10	G	G1	12	5	0.05	0.1	0.05	1
11	G	G1	35	2.3	0.5	0.8	0.6	1
12	G	G1	6.5	4.5	0.7	1	1.0	1
13	G	G1	24	8.5	0.05	0.2	0.16	1
14	G	G1	6.3	4	0.2	0.1	-0.13	1
15	G	G1	19.5	6	0.05	0.2	0.16	1
16	G	G1	17	8	0.05	0	-0.05	0
17	G	G1	13	7.25	0.05	0.1	0.05	0
18	G	G1	6	5.5	0.2	0.9	0.88	0
19	G	G1	6	3.25	0.2	1	1.0	0
20	G	G1	13	4.5	0.9	1	1.0	1
21	G	G2	37	13	0.4	0.6	0.33	1
22	G	G2	2.9	7.75	0.3	0.7	0.57	1
23	G	G2	20	10.5	0.1	0.1	0.0	0
24	G	G2	21.5	8.25	0.05	0.2	0.16	0
25	G	G2	20	11	1	1	0.0	1
26	G	G2	19	11.5	0.8	0.9	0.5	1
27	G	G2	9	6.25	0.05	0.1	0.05	0
28	G	G2	11.5	7.25	0.1	0.9	0.89	0
29	G	G2	13	8.5	0.05	0.2	0.16	0
30	G	G2	12.5	9.5	0.1	0.2	0.11	0
31	G	G2	13	7	0.05	0.2	0.16	0
32	G	G2	5	5.5	0.05	0	-0.05	0
33	G	G2	16	8.5	0.2	1	1.0	0
34	G	G2	31	9.25	0.5	0.5	0.0	1
35	G	G2	17	9.5	0.3	0.4	0.14	0
36	G	G2	17.5	8.75	0.2	0.4	0.25	0
37	G	G2	13	8	0.05	0.1	0.05	0
38	G	G2	22	10.5	0.6	0.8	0.5	0
39	G	G2	19.5	11.5	0.2	0.2	0.0	0
40	G	G2	20	11	0.5	0.5	0.0	1

41	G	G2	26	12.5	0.8	0.9	0.5	1
42	G	G2	22	12	0.7	0.7	0.0	1
43	G	G2	26	14.5	0.9	1	1.0	1
44	G	G2	30	11	0.2	0.4	0.25	1
45	G	G3	24.5	10.25	0.4	0.3	-0.17	1
46	G	G3	14	6.5	0.1	0.1	0.0	1
47	G	G3	20.25	8	0.2	0.2	0.0	0
48	G	G3	12.5	7	0.7	0.5	-0.67	1
49	G	G3	19.75	9.5	0.05	0.4	0.37	1
50	G	G3	19	7	0.1	0.2	0.11	1
51	G	G3	12.75	7.5	0.4	0.3	-0.17	1
52	G	G3	17.75	7.5	0.1	0.3	0.22	0
53	G	G3	14	8.5	0.2	0.2	0.0	0
54	G	G3	18	9	0.8	0.8	0.0	1
55	G	G3	27	8.5	0.1	0.3	0.22	1
56	G	G3	24.5	9.5	0.6	0.3	-0.75	1
57	G	G3	24	10	0.8	1	1.0	1
58	G	G3	14	7.75	0.1	0.3	0.22	1
59	G	G3	19	9	0.8	0.7	-0.5	1
60	G	G3	19	10	0.3	0.6	0.43	1
61	G	G3	29	13.5	0.3	0.6	0.43	1
63	G	G3	37.25	12	0.05	0.5	0.48	1
64	G	G3	26.5	10.5	0.05	0.3	0.26	0
65	G	G3	20.5	8.5	0.9	0.9	0.0	1
66	G	G3	24	9	0.9	1	1.0	1
67	G	G3	17	9	0.8	0.9	0.5	1
68	G	G3	19.75	12	0.3	0.7	0.57	1
69	G	G3	23	7.5	0.7	1	1.0	1
70	G	G3	15.75	8.5	0.7	0.8	0.33	1
71	G	G4	25	8	0.05	0.5	0.47	1
72	G	G4	18.5	8	0.3	0.8	0.71	1
73	G	G4	26	10	0.05	0.4	0.37	1
74	G	G4	27.5	9.75	0.05	0.5	0.47	1
75	G	G4	24.5	8	0.2	0.5	0.38	1
76	G	G4	25	8.75	0.1	0.5	0.44	1
77	G	G4	32	8.5	0.05	0.2	0.16	1
78	G	G4	20	8.75	0.3	0.5	0.29	1
79	G	G4	26	9.5	0.5	0.4	-0.2	1
80	G	G4	13	6.5	0.7	0.8	0.33	1
81	G	G4	22	8	0.8	1	1.0	1
82	G	G4	15.5	7	0.3	0.7	0.57	1
83	G	G4	26	8	0.5	0.7	0.4	1
84	G	G4	23	6	0.5	1	1.0	1
85	G	G4	24.5	7.5	0.1	0.4	0.33	1
86	G	G4	24	9.5	0.2	0.6	0.5	1
87	G	G4	34	6.5	0.4	0.6	0.33	1
88	G	G4	26.75	9	0.05	0.3	0.26	1
89	G	G4	21.75	8	0.1	0.2	0.11	1
90	G	G4	27.5	8.5	0.9	0.9	0.0	1
91	G	G4	31	8.5	0.2	0.3	0.13	1
92	G	G4	37.5	10.75	0.05	0.3	0.26	1
93	G	G4	24.5	9	0.05	0.2	0.16	1
94	G	G4	28.5	8	0.05	0.6	0.58	1
95	G	G4	19.75	10	0.8	0.9	0.5	1
96	G	G4	15.5	7	0.7	0.9	0.67	1
97	G	G4	23.5	7.25	0.9	1	1.0	1
C1	C	C1	28.01	8.8	0	0.1	0.1	1
C2	C	C1	13.69	7.5	0	0.05	0.05	1
C3	C	C1	18.46	7.6	0	0	0.0	1
C4	C	C1	32.15	8.5	0	0	0.0	1
C5	C	C1	28.97	8.5	0	0.1	0.1	1
C6	C	C2	25.15	12.5	0	0.05	0.05	1
C7	C	C2	20.69	11.6	0	0.05	0.05	1
C8	C	C2	13.69	7.2	0	0	0.0	1
C9	C	C2	27.69	12.3	0	0.05	0.05	1
C10	C	C2	34.7	13.2	0	0.1	0.1	1
C11	C	C3	25.46	11.6	0	0.2	0.2	1
C12	C	C3	25.46	9.25	0	0.2	0.2	1
C13	C	C3	19.42	8.25	0	0.1	0.1	1
C14	C	C3	14.64	8.25	0	0.1	0.1	1
C15	C	C3	27.69	9.1	0	0.05	0.05	1
C16	C	C4	33.74	11.25	0	0	0.0	1
C17	C	C4	28.01	13.6	0	0.1	0.1	1
C18	C	C4	23.87	12.6	0	0	0.0	1
C19	C	C4	38.52	13	0	0	0.0	1
C20	C	C4	28.01	9.9	0	0.05	0.05	0

Appendix 2.

Soil nutrients and properties

Table A2. Estimated regression parameters for the generalised linear model comparing soil nutrients and properties between asymptomatic and symptomatic sites.

Variable	Estimate (symptomatic sites)	SE	z-value ^a	P-value ^b
pH	0.9562	1.0119	0.945	0.345
Ca	0.0011	0.0010	1.191	0.234
P	0.5333	0.8981	0.594	0.553
K	0.0281	0.0607	0.462	0.644
Inorganic N	0.1472	0.2206	0.667	0.505
NH ₄ ⁺ -N	0.1498	0.2305	0.650	0.516
NO ₃ ⁻ -N	4.1701	5.5492	0.751	0.452
Loss on ignition	0.0478	0.0696	0.686	0.493
Water-holding capacity	0.0162	0.0188	0.864	0.388

^a Estimate/SE

^b Significant P-values indicated by asterisks (***) < 0.001 < ** < 0.01 < * < 0.05 < . < 0.1)

Table A3. Estimated regression parameters for the generalised linear model comparing soil nutrients and properties between healthy trees (group GH+CH) and affected trees (group GA).

Variable	Estimate (healthy trees)	SE	z-value ^a	P-value ^b
pH	0.6778	0.9821	0.690	0.490
Ca	0.0005	0.0006	0.811	0.417
P	-0.2021	0.7222	-0.280	0.780
K	0.0313	0.0553	0.566	0.572
Inorganic N	0.0718	0.2011	0.357	0.721
NH ₄ ⁺ -N	0.0619	0.2119	0.292	0.770
NO ₃ ⁻ -N	4.5720	4.2204	1.083	0.279
Loss on ignition	-0.0185	0.0417	-0.444	0.657
Water-holding capacity	-0.0002	0.0101	-0.023	0.981

^a Estimate/SE

^b Significant P-values indicated by asterisks (***) < 0.001 < ** < 0.01 < * < 0.05 < . < 0.1)

Table A4. Estimated marginal means for the linear mixed-effects model testing differences in soil properties between group types (CH – asymptomatic sites, asymptomatic trees; GA – symptomatic sites, symptomatic trees; GH – symptomatic sites, asymptomatic trees). No results were significant.

Variable	Contrast ^a	Estimate	SE	df ^b	t-ratio ^c	P-value ^d
pH	CH - GA	-0.448	0.509	2	-0.879	0.7017
	CH - GH	-0.333	0.509	2	-0.653	0.8098
	GA - GH	0.115	0.131	2	0.876	0.7034
Ca	CH - GA	-852	726	2	-1.175	0.5687
	CH - GH	-687	726	2	-0.947	0.6696
	GA - GH	165	456	2	0.362	0.9328
P	CH - GA	-0.13	0.709	2	-0.183	0.9818
	CH - GH	-0.58	0.709	2	-0.818	0.7308
	GA - GH	-0.45	0.530	2	-0.850	0.7157
K	CH - GA	-4.62	8.76	2	-0.527	0.8673
	CH - GH	-1.61	8.76	2	-0.184	0.9818
	GA - GH	3.01	7.88	2	0.382	0.9258
Inorganic N	CH - GA	-1.2803	2.41	2	-0.531	0.8656
	CH - GH	-1.2325	2.41	2	-0.511	0.8742
	GA - GH	0.0478	1.68	2	0.029	0.9996
NH ₄ ⁺ -N	CH - GA	-1.1175	2.29	2	-0.487	0.8844
	CH - GH	-1.2050	2.29	2	-0.525	0.8681
	GA - GH	-0.0875	1.57	2	-0.056	0.9983
NO ₃ ⁻ -N	CH - GA	-0.1628	0.140	2	-1.160	0.5747
	CH - GH	-0.0275	0.140	2	-0.196	0.9792
	GA - GH	0.1353	0.119	2	1.137	0.5846
Loss on Ignition	CH - GA	-2.62	13.9	2	-0.188	0.9808
	CH - GH	-15.70	13.9	2	-1.129	0.5881
	GA - GH	-13.07	11.9	2	-1.102	0.5998
Water-holding capacity	CH - GA	-23.4	45.9	2	-0.510	0.8746
	CH - GH	-48.6	45.9	2	-1.059	0.6188
	GA - GH	-25.2	33.2	2	-0.758	0.7597

^a Pairwise comparison

^b Degrees of freedom

^c Estimate/SE

^d Significant P-values indicated by asterisks (*** < 0.001 < ** < 0.01 < * < 0.05 < . < 0.1)

Soil properties – principal component analyses

Principal component analysis (PCA) plots illustrating the relatedness between the site types (G – symptomatic, C – asymptomatic, Fig. A1) and between the group types (CH – asymptomatic sites, asymptomatic trees; GA – symptomatic sites, symptomatic trees; GH – symptomatic sites, asymptomatic trees; Fig. A2) regarding soil nutrients and properties.

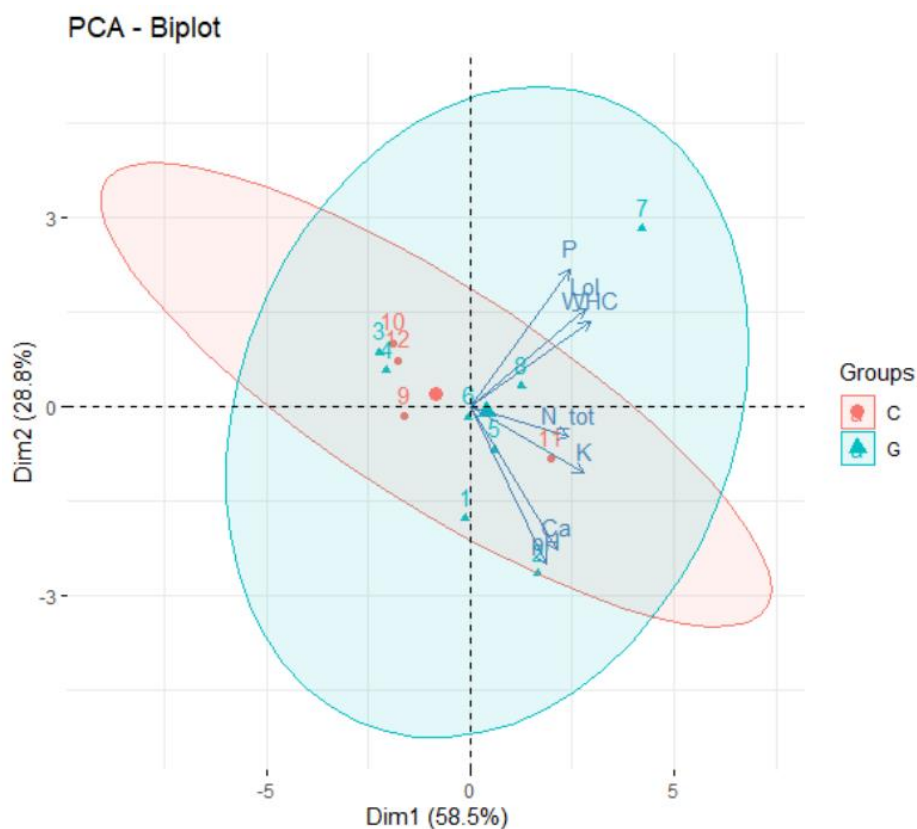


Figure A1. The relatedness between symptomatic (G) and asymptomatic (C) sites regarding soil nutrients and properties visualised by a principal component analysis (PCA) plot. The size and width of the ellipses reveal a large variance within the site types, although the asymptomatic sites (C) are more united than the symptomatic sites (G). The plot also shows a clear correlation between phosphorus, loss on ignition and water-holding capacity, between total nitrogen and potassium, and between pH and calcium (blue arrows). The asymptomatic site C3 (#11 in the plot) diverges from other asymptomatic sites.

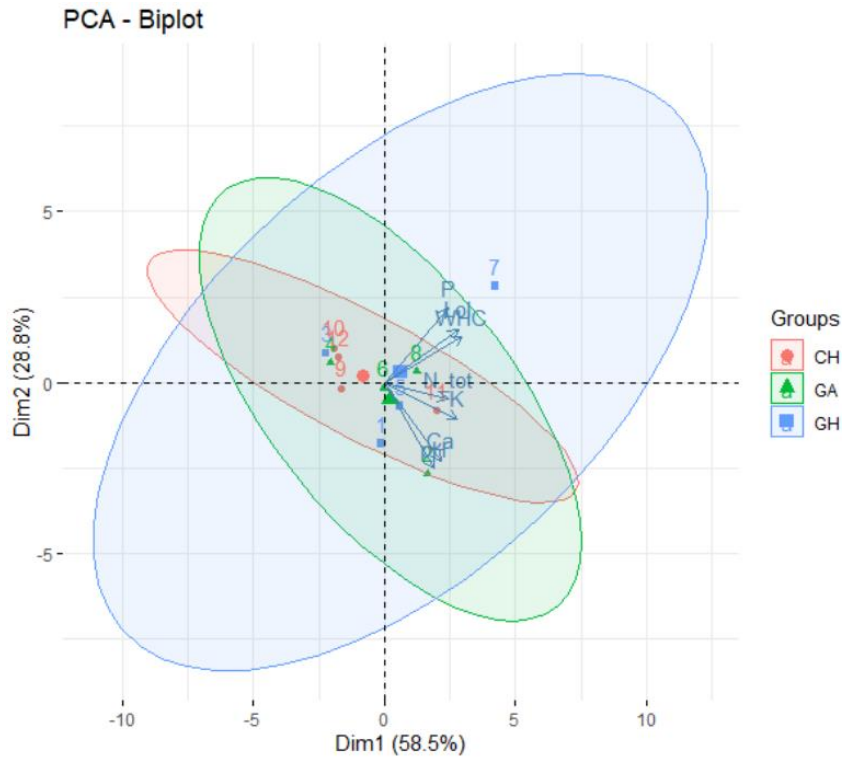


Figure A2. The relatedness between the group types (CH (asymptomatic sites – asymptomatic trees), GA (symptomatic sites – symptomatic trees), GH (symptomatic sites – asymptomatic trees)) regarding soil nutrients and properties visualised by a principal component analysis (PCA) plot. The size and width of the ellipses reveal a large variance within the group types, although members of group CH are more united than members of the other groups. The plot also shows a clear correlation between phosphorus, loss on ignition and water-holding capacity, between total nitrogen and potassium, and between pH and calcium (blue arrows).